The Sampling Pattern Cube

A Framework for Representation and Evaluation of Plenoptic Capturing Systems

Mitra Damghanian

Department of Information and Communication Systems
Faculty of Science, Technology and Media
Mid Sweden University

Licentiate Thesis No. 99
Sundsvall, Sweden
2013

Mittuniversitetet
Avdelningen för informations-och kommunikationssystem
Fakulteten för naturvetenskap, teknik och medier
ISBN 978-91-87103-73-5
ISSN 1652-8948
SE-851 70 Sundsvall
SWEDEN

Akademisk avhandling som med tillstånd av Mittuniversitetet framlägges till offentlig granskning för avläggande av teknologie licentiatexamen tisdagen den 4 juni 2013 i L111, Mittuniversitetet, Holmgatan 10, Sundsvall.

Tryck: Tryckeriet Mittuniversitetet

To My Family
In a time of destruction, create something

Abstract

Digital cameras have already entered our everyday life. Rapid technological advances have made it easier and cheaper to develop new cameras with unconventional structures. The plenoptic camera is one of the new devices which can capture the light information which is then able to be processed for applications such as focus adjustments. The high level camera properties, such as the spatial or angular resolution are required to evaluate and compare plenoptic cameras. With complex camera structures that introduce trade-offs between various high level camera properties, it is no longer straightforward to describe and extract these properties. Proper models, methods and metrics with the desired level of details are beneficial to describe and evaluate plenoptic camera properties.

This thesis attempts to describe and evaluate camera properties using a model based representation of plenoptic capturing systems in favour of a unified language. The SPC model is proposed and it describes which light samples from the scene are captured by the camera system. Light samples in the SPC model carry the ray and focus information of the capturing setup. To demonstrate the capabilities of the introduced model, property extractors for lateral resolution are defined and evaluated. The lateral resolution values obtained from the introduced model are compared with the results from the ray-based model and the ground truth data. The knowledge about how to generate and visualize the proposed model and how to extract the camera properties from the model based representation of the capturing system is collated to form the SPC framework.

The main outcomes of the thesis can be summarized in the following points: A model based representation of the light sampling behaviour of the plenoptic capturing system is introduced, which incorporates the focus information as well as the ray information. A framework is developed to generate the SPC model and to extract high level properties of the plenoptic capturing system. Results confirm that the SPC model is capable of describing the light sampling behaviour of the capturing system, and that the SPC framework is capable of extracting high level camera properties with a higher descriptive level as compared to the ray-based model. The results from the proposed model compete with those from the more elaborate wave optics model in the ranges that wave nature of the light is not dominant. The outcome of the thesis can benefit design, evaluation and comparison of the complex capturing systems.

Keywords: Camera modelling, plenoptic camera, lateral resolution.

Acknowledgements

Concluding the recent two years of my journey, I'm grateful that I had the chance to explore a new area, which helped me to get a wider view both in science and life. It has been a new experience, in a totally new place, full of challenges and spiced with cultural contrasts, and I loved it because of all those.

My special thanks to my supervisors Mårten Sjöström and Roger Olsson, whom I learned from more than they can ever know, for their excellent support in all research matters and for their trust in me. I would like to thank my colleagues at the Department of Information and Communication Systems and especially in the Realistic 3D research group. Thanks to Sebastian Schwarz, Suryanarayana Muddala and Yun Li for being there for me. Thanks to Annika Berggren for her kind assistance in all organizational matters. And thanks to Fiona Wait for proofreading the text.

Finally I want to thank my family; their smile is enough to give me all the courage I need.

Table of Contents

List of Papers

This monograph is mainly based on the following papers, herein referred by their Roman numerals:

I Mitra Damghanian, Roger Olsson and Mårten Sjöström. The sampling pattern cube a representation and evaluation tool for optical capturing systems In *2012 Advanced Concepts for Intelligent Vision Systems*, Lecture Notes in Computer Science 7517, 120-131, Springer Berlin Heidelberg, 2012.

II Mitra Damghanian, Roger Olsson and Mårten Sjöström. Extraction of the lateral resolution in a plenoptic camera using the SPC model. In *2012 International Conference on 3D Imaging IC3D*, IEEE, Liège, Belgium, 2012.

III Mitra Damghanian, Roger Olsson, Mårten Sjöström, Hèctor Navarro Fructuoso and Manuel Martinez Corral. Investigating the lateral resolution in a plenoptic capturing system using the SPC model. In *2013 Electronic Imaging Conference-Digital Photography IX*, 86600T-86600T-8, IS&TSPIE, Burlingame, CA, 2013.

List of Figures

List of Tables

Terminology

Abbreviations and Acronyms

CCD	Charge Coupled Device
CFV	Common Field of View
CG	Computer Graphics
CMOS	Complementary Metal Oxide Semiconductor
DoF	Depth of Field
LC	Light Cone
MTF	Modulation Transfer Function
OTF	Optical Transfer Function
PC	Plenoptic Camera
PF	Plenoptic Function
PTF	Phase Transfer Function
PSF	Point Spread Function
SPC	Sampling Pattern Cube

Mathematical Notation

α	Lenslet viewing angle
Δz	The depth range in which objects are accurately reconstructed
θ	The angle between the ray and the optical axis in y direction
θ_s	The start of the angular span of the light cone in y direction
θ_f	The ending of the angular span of the light cone in y direction
λ	The wavelength
ϕ	The angle between the ray and the optical axis in x direction
ϕ_s	The start of the angular span of the light cone in x direction
ϕ_f	The ending of the angular span of the light cone in x direction
ξ	Spatial frequency in the x-plane
η	Spatial frequency in the y-plane
$A[\cdot]$	Aperture operator
a	Object distance to the optical centre

$B[\cdot]$	Base operator
b	Image distance to the optical centre
C_i	The light cone number i
d_L	Hyperfocal distance
d_e	Euclidean distance
F	Focal length of the main lens
$\hat{F}(.)$	The Fourier transformation
f	Focal length of the lenslet
g	The spacing between lenslet array and the image sensor
I	Light intensity
i	An integer
k	An integer
$L[\cdot]$	Lens operator
min_dist	The maximum size line piece created by the overlapping span of the LCs in the depth plane of interest
n	Refractive index
p	The dimension of the angular span in the **q-p** representation
pps	The projected pixel size in the depth plane of interest
q	The dimension of the position in the **q-p** representation
(q, p)	A plane in the **q-p** representation
q-p	A two dimensional position-angel representation space
R	Resolution of the image sensor
r	An integer
R_s	Spatial resolution at the image plane
Res_lim	Lateral resolution limit
$S[\cdot]$	Split operator
(s, t)	Arbitrary plane in parallel with the (x, y) plane
t	Time variable
(u, v)	Arbitrary plane in parallel with the (x, y) plane
w	Width of the base of the light cone
x	The first dimension in Cartesian coordinate system
(x, y, z)	The Cartesian coordinate system
(x, y, z)	A point in Cartesian coordinate system
y	The second dimension in Cartesian coordinate system
z	The depth dimension; as a plane, the plane with a normal vector in the **z** direction

Chapter 1

Introduction

Cameras have changed the way we live today. They are integrated into many devices ranging from tablets and mobile phones to vehicles. Digital cameras have become a part of our everyday life aided by the rapidly developing technology; these handy devices are becoming cheaper and are providing even more built-in features. Digital photography has made it easy in relation to capturing, sending and storing high quality images all at a reasonable price.

In addition to conventional cameras that have become very popular and for which there are an enormous number, unconventional capturing systems are also being developed faster than ever based on the current technological advances. At the present time, it is becoming economically more feasible to build camera arrays because of the lower costs for the cameras as well as the electronics required for storing and processing the huge data sets as the output of those camera arrays. In addition to the feasibility of multi-camera capture setups, the emergence of plenoptic cameras (PCs) has been observed. Plenoptic cameras have been developed and have progressed into the product market during recent years [1, 2, 3], as another example of unconventional camera systems. Plenoptic cameras capture the light information that can be processed at a later stage for applications such as focus adjustments, depth of field extension and more. As the technology developments have provided opportunities for various types of capturing systems for different applications, the expectation is that there will also be more innovative capture designs in the future.

Cameras have a wide range of properties to suit diverse applications. This fact can cause uncertainties in relation to making the correct choice for the desired capturing system. Unconventional capturing setups do not assist in making that decision easier as they add to the ambiguity in relation to the description of the camera parameters, as well as introducing new trade-offs in the properties space. Camera evaluation is naturally an application dependant question [4]. To convey this evaluation, one method used is to look at the multi-dimensional camera property space (see Figure 1.1). However, having knowledge of the desired camera properties remains the key feature in designing or choosing the correct capturing solution. As a capturing system designer, one would also like to have knowledge of the effect of

variations or design tolerances in the capturing system parameters on the high level properties of the camera system.

Computational photography is another interesting field related to the imaging technology and this is also developing at a rapid pace at the present time [5, 6, 7]. This field has enhanced the capabilities of the digital photography by introducing and implementing image capturing, processing, and manipulation techniques. Computational photography provides the opportunity to capture an image now and to modify the properties such as depth of field at a later stage. Unconventional cameras do provide the required information for such adjustments. Though computational photography is a powerful tool, it has introduced complexities to the terms which have been previously easy to define and be derived from the cameras.

With complex camera structures such as plenoptic cameras, in addition to the popularity of the computational photography techniques, it is no longer straightforward to describe and extract the high level properties of the capturing systems, which are required to evaluate a capturing setup and to make meaningful comparisons between different capturing setups [8, 9, 10].

In the context of the plenoptic capturing setups, one solution for extracting those high level camera properties is basically by conducting practical measurements, which, naturally, is an elaborate though costly solution for many applications. Moreover, the intended or unintended variations in the plenoptic capturing setup will require a new set of measurements to be conducted. To ease the process, models are utilized which describe the system with the desired level of details.

The knowledge concerning how the light is captured (sampled) by the image capturing system is crucial for extracting the high level properties of the capturing system. Thus proper models for light and the capturing system are essential to describe the light sampling behaviour of the system. Existing models are different in their complexity as well as their descriptive level and thus each model becomes suitable for a range of applications.

1.1 Motivation

Established capturing properties such as image resolution are required to be described thoroughly in complex multi-dimensional capturing setups such as plenoptic cameras, as they introduce a trade-off between properties [4] such as the resolution, depth of field and signal to noise ratio [8, 9, 10]. These high-level properties can be inferred from in-depth knowledge regarding how the image capturing system samples the radiance through points in three-dimensional space. This investigation is required, not only to understand trade-offs among various capturing properties between unconventional capturing systems, but also to explore each system's behaviour individually. Adjustments in the system or unintended variations in the capturing system properties are other sources of variation in the sampling behaviour and so in the high-level properties of the system.

Models are therefore a valuable means in order to understand the capturing sys-

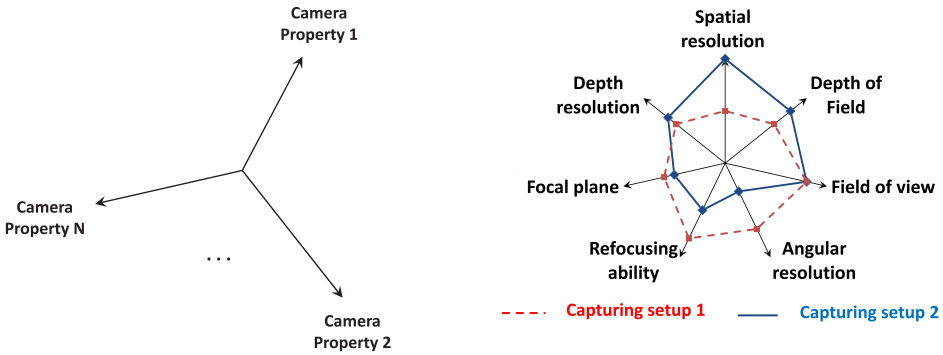

(a) Multi-dimensional camera properties space

(b) Example

Figure 1.1: A graphical representation of the multi-dimensional space of the capturing system properties (a) Illustrating the concept (b) An example for comparing two capturing systems in the multi-dimensional properties space

tem regarding its potential and limitations, facilitating the development of more efficient post-processing algorithms and insightful system manipulations in order to obtain the desired system features. This knowledge can also be used for developing, rendering and post processing approaches or adjusting prior computational methods for new device setups. In this context, models, methods and metrics that assist exploring and formulating this trade-off are highly beneficial for study as well as in relation to the design of plenoptic capturing systems.

Capturing systems sample the light field in various ways which result in different capturing properties and trade-offs between those properties. Models have been proposed that describe the light field and how it is sampled by different image capturing systems [11, 12]. Previously proposed models range from simple ray-based geometrical models to complete wave optics simulations, each with a different level of complexity and varying explanatory levels in relation to the system's capturing properties. The light field model, which is a simplified representation of the plenoptic function (with one less dimension), has proven useful for applications spanning computer graphics, digital photography, and 3D reconstruction [13]. However, models applied to the plenoptic capturing systems are desired to have low complexity as well as a high descriptive level within their scope. It is beneficial to have a model that provides straightforward extraction of features with a desired level of details, when analyzing, designing and using plenoptic capturing systems. At the moment, not all of these demands have been fulfilled with the existing models and metrics which provides room for novelties and improvements in the field.

The desire for a unified language in describing the camera properties and the lack of such frameworks is another drive for developing new models [4]. Terms

such as ”Mega-rays” to describe resolution in a plenoptic capturing system does not provide a clear figure of the spatial resolution of the capturing system in the depth plane of interest, which might first come to mind on hearing the term ”resolution”. It also does not provide a basis for a comparison of one capturing system with other capturing systems. Although the technology has made it cheaper and faster for unconventional cameras as well as multi-camera capture setups to emerge and to be developed, it has not become easier to make decisions regarding a specific capturing set-up. To do so, a user must have the means to compare properties and features provided by each capture setup. The technology developers will also benefit from being able to clearly express the properties of their offered solutions. A unified descriptive language can assist in removing such ambiguity surrounding different terms, as these are describing the high level properties of the plenoptic camera setups, as well as facilitating meaningful comparisons between different plenoptic capturing systems.

1.2 Problem definition

The aim of this work is to introduce a framework for the representation and evaluation of plenoptic capturing systems in favour of a unified language for extracting and expressing camera trade-offs in a multi-dimensional camera properties space (see Figure 1.1). The work presented in this thesis is based on the following verifiable goals:

1. To introduce a model:
    - Representing the light sampling behaviour of plenoptic image capturing systems.
    - Incorporating the ray information as well as the focus information of the plenoptic image capturing system.
2. To build a framework based on the introduced model which is capable of extracting the high level properties of plenoptic image capturing systems.

In the presented work, complex capturing systems, namely plenoptic cameras and their properties are being considered. The camera properties excluded from the scope of this work are those caused by the wave nature of light such as diffraction and polarization.

1.3 Approach

To fullfil the aim of this thesis work, the sampling pattern cube (SPC) framework is introduced. The SPC framework is principally a system of rules describing how to relate the physical capturing system parameters to a new model representation

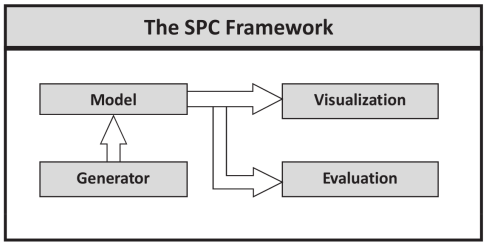

Figure 1.2: A graphical illustration of the framework and model subject of this thesis work, for representation and evaluation of plenoptic capturing systems

of the system, and, following this, how to extract the high level properties of the capturing system from that model. The SPC model is the heart of the introduced framework for the representation and evaluation of plenoptic capturing systems. In a top down approach, the SPC framework is divided into smaller modules. These modules, including the model, the model generator, the visualization and the evaluation module, all interact towards the aim of this thesis work. Figure 1.2 gives a graphical representation of the modules in the SPC framework and how they relate to each other.

The SPC framework is also interacting with the outside world. It receives parameters related to the capturing setup (the camera structure) and provides outputs in the form of visualization results and camera properties. Figure 1.3 illustrates the interaction of the different modules in the SPC framework with the outside world. Figure 1.3 also provides additional information about different modules in the framework while a detailed description of each module and its components is given in Chapters 3, 4 and 5.

1.4 Thesis outline

Chapter 2 will briefly provide the required background information. It will cover the basic knowledge about capturing systems, in particular the plenoptic setup which is the focus of this work. Optical models including those utilized in computational photography are dealt with briefly in Chapter 2 which will provide knowledge about how to relate the current work with other available models. The details concerning the proposed SPC model are provided in Chapter 3 and a description regarding the generation of the SPC model using the model generator module in the SPC framework is presented. Chapter 4 provides an elaboration regarding the visualization module in the SPC framework. It illustrates how it is possible to visualize the SPC model and how to benefit from this visualization. Discussion concerning the proposed framework will continue in Chapter 5 and it is at this point that property extractors are introduced in order to empower the evaluation module. The SPC model is evaluated in Chapter 6 by applying the introduced property extractors to plenoptic capturing setups and comparing the results with those from established models.

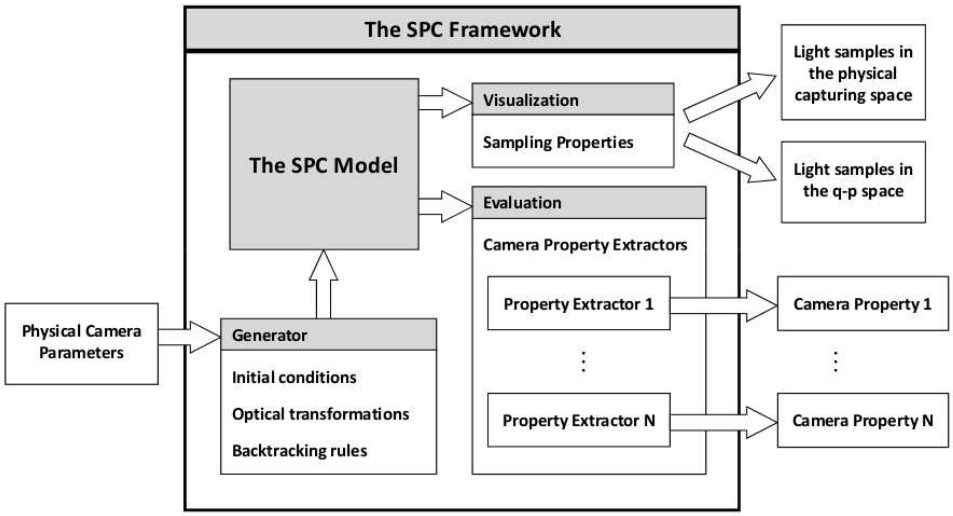

Figure 1.3: A graphical illustration of the inputs and outputs of the framework subject of this thesis work

Finally, in Chapter 7 the work is concluded and possible future developments are discussed.

1.5 Contributions

The content of this thesis work is mainly based on the previously listed papers I to III. The contributions can be divided into three main parts:

1. A model that describes the light sampling properties of a plenoptic capturing system and the instructions and rules for building that model.
2. A property extractor that is capable of extracting the lateral resolution of a plenoptic camera leveraging on the focal properties of the capturing system preserved in the provided model.
3. Introducing and developing a framework for modelling complex capturing systems such as plenoptic cameras and extracting the high level properties of the capturing system with the desired level of details.

Chapter 2

Light Models and Plenoptic Capturing Systems

This chapter provides the required material and the background information for the remainder of this thesis work. The chapter is started by means of an introduction to optical models with different complexity and descriptive levels. The plenoptic function and its practical subsets are then provided, which then leads on to the topic of the plenoptic cameras as the main focus. The plenoptic camera structure and intrinsic trade-offs in this capturing configuration will be discussed, and a short summary will conclude this chapter.

2.1 Optical models

Optics is the branch of physics which involves the behaviour and properties of light, including its interactions with matter, and the construction of instruments that use or detect it. Different optical models with various complexity levels are exploited for describing various light properties in different domains and applications. A correct choice of optical model is necessary in order to achieve the desired level of explanation from the model for a reasonable computational cost.

2.1.1 Geometrical optics

Geometrical optics, or ray optics, describes the propagation of light in terms of rays which travel in straight lines, and whose paths are governed by the laws of reflection and refraction at the interfaces between different media [14].

Reflection and refraction can be summarised as follows: When a ray of light hits the boundary between two transparent materials, it is divided into a reflected and a refracted ray. The law of reflection states that the reflected ray lies in the plane

of incidence, and the angle of reflection equals the angle of incidence. The law of refraction states that the refracted ray lies in the plane of incidence, and that the sine of the angle of refraction divided by the sine of the angle of incidence is a constant:

$$\frac{\sin\theta_1}{\sin\theta_2} = n, \tag{2.1}$$

where n is a constant for any two materials and a given colour (wavelength) of light. This is known as the refractive index. The laws of reflection and refraction can be derived from the principle which states that the path taken between two points by a ray of light is the path that can be traversed in the least time [15].

Geometric optics is often simplified by making a paraxial approximation, or a small angle approximation. Paraxial approximation is a method of determining the first-order properties of an optical system that assumes all ray angles are small and thus:

$$\begin{aligned}\sin\theta &\approx \theta,\\ \tan\theta &\approx \theta,\\ \cos\theta &\approx 1,\end{aligned}$$

where θ is the smallest angle between the ray and the optical axis. A paraxial ray-trace is linear with respect to ray angles and heights [16]. However, careful consideration should be given as to where this approximation is valid as this depends on the optical system configuration.

2.1.2 More elaborated optical models

Interference and diffraction are not explained by geometrical optics. More elaborated optical models such as the wave optics (sometimes called the physical optics model) and the quantum optics model are those covering a wider range of the behaviour and properties of light. The debate about the nature of light and the wave-particle duality as the best explanation for a broad range of observed phenomena is still ongoing in modern physics. The complexity of the model can be estimated from the level of complexity of the light elements in each model and the methods used to work with the light elements. Table 2.1 provides a brief comparison between the geometrical model, the wave optics and the quantum optics model in order to offer an idea regarding the different complexity levels. The point is that in order to describe a wider range of phenomena, a more extensive model of the physical concept (light here) is necessary. But the desire is to add the minimum complexity while providing the maximum benefit. Details about these elaborate optical models can be found in standard optics books. However, a few points will now be mentioned in brief which will be used at a later stage in this thesis work.

One clear distinction between the geometrical optics and the wave optics model is the concept of optical transfer function (OTF) in the latter. The optical transfer function is the frequency response of that optical system. Considering the imaging

Table 2.1: Comparison of the optical models, higher descriptive level comes with the higher complexity in the model

Optical Model	Light Element	Method	Application
Geometrical Optics	Light rays	Paraxial approximation, disregarding wavelength	Ray tracing, digital photography
Wave Optics	Electromagnetic Wave fields	Maxwell equations, harmonic waves, Fourier-theory	Interference, diffraction, polarization, holography
Quantum Optics	Particles (photons)	Planck's radiation law, quantum mechanics	Photo-electric effect, Kerr-effect, Faraday-effect, laser

system as an optical system, the OTF is the amplitude and phase in the image relative to the amplitude and phase in the object as a function of frequency, when the system is assumed to respond linearly and to be space invariant [17]. The magnitude component (light intensity) of the OTF is known as the modulation transfer function (MTF), and the phase part is known as the phase transfer function (PTF):

$$OTF(\xi, \eta) = MTF(\xi, \eta) \exp(i \cdot PTF(\xi, \eta)), \tag{2.2}$$

where ξ and η are the spatial frequency in the x- and y-planes, respectively. The spatial domain representation of the MTF (which is in the frequency domain) is called the point spread function (PSF), see Equation 2.3. The point spread function describes the response of an imaging system to a point light source. In the language of system analysis, the optical system is a two dimensional, space invariant, fixed parameter linear system and the PSF is its impulse response. The spatial domain and the frequency domain are related using:

$$MTF = \hat{F}(PSF), \tag{2.3}$$

where $\hat{F}(.)$ is showing the Fourier transformation.

Ray-based models of light have been utilized for computer graphics and computer vision. Some early excursions into the wave optics models by Gershon Elber [18] proved computationally intense, and thus the pinhole-camera and ideal-thin-lens models of optics have been considered adequate for computer graphics use [19]. However, the ray-based models were sometimes extended with special-case models e.g. for diffraction [20], which cannot be properly handled using the ray-based models alone. Other examples are the surface scattering phenomena and developing proper reflection models, which demand more than a purely ray-based model.

2.2 Plenoptic function

The concept of plenoptic function (PF) is restricted to geometric optics and so the fundamental light carriers are in the form of rays. Geometric optics is applied to the domain of incoherent light and to objects larger than the wavelength of light, which is well matched with the scope of this thesis work.

The plenoptic function is a ray-based model for light that includes the colour spectrum as well as spatial, temporal, and directional variations [21]. The plenoptic function of a 3D scene, introduced by Adelson and Bergen [22], describes the intensity of all irradiance observed at every point in the 3D scene, coming from every direction. For an arbitrary dynamic scene, the plenoptic function is of dimension seven [23]:

$$PF(x, y, z, \phi, \theta, \lambda, t) = I, \tag{2.4}$$

where I is the light intensity of the incoming light rays at any spatial 3D-point (x, y, z) from any direction given by spherical coordinates (ϕ, θ) for any wavelength λ at any time t. If the PF is known to its full extent, then it is possible to reproduce the visual scene appearance precisely from any view point at any time. Unfortunately, it is technically not feasible to record an arbitrary PF of full dimensionality. The problem is simplified in relation to a static scene, which removes the time variable t. Another simplification is according to the λ values, which are discredited into the three primary colours red, green and blue. Based on the human tristimulus colour perception, the discritized λ values can be interpolated to cover the range of perceptible colours.

In conventional 2D imaging systems, all the visual information is integrated over the dimensions of the PF with the exception of a two dimensional spatially varying subset. The result of this integration is the conventional photograph. The integration occurs due to the nature of the digital light sensors (either CCD or CMOS) and the information loss is irreversible.

Based on the above definition of the plenoptic function, it is possible to relate plenoptic imaging to all those imaging methods which preserve the higher dimensions of the plenoptic function compared to a conventional photograph. Since these dimensions are the colour spectrum, spatial, temporal, and directional variations, the plenoptic image acquisition approaches include the wide range of methods preserving either of those dimensions using a variety of capturing setups such as single shot, sequential and multi-device capturing setups. However, the plenoptic cameras in the scope of this thesis work are those which prevent the averaging of the radiance of the incident light rays in a sensor pixel by introducing spatio-angular selectivity. The specific structure of a plenoptic camera will be described in more details in Section 2.5.

2.3 Light field

The plenoptic function of a given scene contains a large degree of redundancy. Sampling and storing the full plenoptic dimensional function for any useful region of space is impractical. Since the radiance of a given ray does not change in free space, the plenoptic function can be expressed with one less dimension as a light field in a region free of occluders [12, 11]. The light field or the modelled radiance can be considered as a density function in the ray space. The light field representation has been utilized to investigate camera trade-offs [9] and has proven useful for applications spanning computer graphics, digital photography, and 3D reconstruction. The scope of the light field has also been broadened by employing wave optics to model diffraction and interference [24] where the resulting augmented light field gains a higher descriptive level at the expense of increased model complexity.

2.3.1 Two plane representation of the light field

The light field (LF) is a 4D representation of the plenoptic function in the region free of occluders. Hence the light field can be parameterized with two coplanar planes (u, v) and (s, t). Each light ray passing through the volume between the planes can be described by its intersection points by $(u, v) - (s, t)$ coordinates. Thus the light field as the 4D representation of the plenoptic function can be written as:

$$LF(u, v, s, t) = I. \tag{2.5}$$

2.3.2 Ray space

Another 4D re-parameterization of the plenoptic function is the ray space [23]. This representation, first introduced in [25], uses a plane in space to define bundles of rays passing through this plane. For the (x, y) plane at $z = 0$ each ray can be described by its intersection with the plane at (x, y) and two angles (θ, ϕ) giving the direction:

$$RS(x, y, \theta, \phi) = I. \tag{2.6}$$

2.4 Sampling the light field

The full set of light rays for all spatial (and angular) dimensions form the full light field (or the full ray space). However, the recording of a full light field is not practically feasible, which makes the sampling process inevitable. Sampling of Equation 2.5 with real sensors introduces discretization on two levels:

1. Angular sampling
2. Spatial sampling

due to the finite pixel resolution of the imaging sensor. It is therefore necessary to obey the sampling theorem to avoid aliasing.

Many researchers have analysed light field sampling [26, 27]. In previous works, models have been proposed that describe the light field and how it is sampled by different image capturing systems [28, 11, 12]. The number and arrangement of images and the resolution of each image are together called the sampling of the 4D light field [13]. Thus different capturing setups result in different samplings of the light field. Since the knowledge regarding how the light field is sampled is closely related to the acquisition method, the light field sampling methods can be classified based on the light field acquisition methods. Some of the light field sampling methods are described here in brief.

2.4.1 Camera arrays (or multiple sensors)

One method for sampling the light field is utilizing an array of conventional 2D cameras distributed on a plane. This method is also referred to as the multi-view technique. Creating the light field from a set of images corresponds to inserting each 2D slice into the 4D light field representation. Considering each image as a two dimensional slice of the 4D light field, an estimate of the light field is obtained from concatenating the captured images. Based on assistance from the two plane notation for the representation of the light field, the camera array capturing method results in the low resolution samples on the (u, v) plane where the camera centres are located, and high resolution samples on the (s, t) or the sensors' plane. The sampling resolution property in this method is closely related to the fact that each camera has a relatively high spatial resolution (high resolution in the (s, t) plane) but the number of cameras is limited (low resolution in the (u, v) plane). A number of methods used for capturing the light field using multi sensor setups are presented in [29, 30, 31].

2.4.2 Temporal multiplexing

Camera arrays cannot provide sufficient light field resolution for certain applications. Sparse light field sampling is a natural result of the camera size which physically limits the camera centres from being located close to each other. Moreover, camera arrays are costly and have high maintenance and engineering complexities. To overcome these limitations, an alternative method is using a single camera capturing multiple images from different view points. Temporal multiplexing or distributing measurements over time are applicable to the static scenes. Examples of such implementations can be found in [12, 11, 32, 33]

2.4.3 Frequency multiplexing

Although temporal multiplexing reduces complexity and cost of the camera array systems, it can only be applied to the static scenes. Thus, other means of multiplexing the 4D light field into a 2D image are required to overcome this limitation. [34]

introduces frequency multiplexing as an alternative method for achieving a single sensor light field capture. Frequency multiplexing method (also referred to as coded aperture) is implemented by placing non-refractive light-attenuating masks slightly in front of a conventional image sensor or outside the camera body near the objective lens. These masks have a Fourier transform of an array of impulses which provide frequency domain multiplexing of the 4D Fourier transform of the light field into the Fourier transform of the 2D sensor image. A number of light field capturing implementations using predefined and adaptive mask patterns for frequency multiplexing can be found in [34, 35, 36, 37].

2.4.4 Spatial multiplexing

Spatial multiplexing produces an interlaced array of elemental images within the image formed on a single image sensor. This method is mostly known as integral imaging, which is a digital realization of the integral photography, introduced by Lippmann [38] in 1908. Spatial multiplexing allows for the light field capture of dynamic scenes but sacrifices spatial sampling in favour of angular sampling as a result of the finite pixel size. One implementation of a spatial multiplexing system to capture the light field, uses an array of microlenses placed near the image sensor. This configuration is called a plenoptic camera (PC) and is closely investigated in Section 2.5. Spatial multiplexing using a single camera is applied when the range of view points spans a short baseline (from inches to microns) [13]. Examples of such implementations can be found in [39, 40].

The spatial multiplexing is not limited to the above mentioned implementations. Adding an external lens attachment with an array of lenses and prisms [41] and the same approach, but with variable focus lenses [42, 43] are two of numerous other schemes using a spatial multiplexing approach for sampling the light field.

2.4.5 Computer graphics method

Light fields can also be created by rendering images from 3D models. If the geometry and the colour information of the scene is known, which is usually the case in computer generated graphics (CG), then standard ray tracing can provide the light field with the desired resolution [27]. However the focus in this thesis work is on light field from photography rather than CG.

2.5 Plenoptic camera

Conventional cameras average radiance of light rays over the incidence angle to a sensor pixel, resulting in a 2D projection of the 4D light field, which is the traditional image. A conventional camera setup is illustrated in Figure 2.1 in a very abstract form. The object, main lens and the image sensor form a relay system:

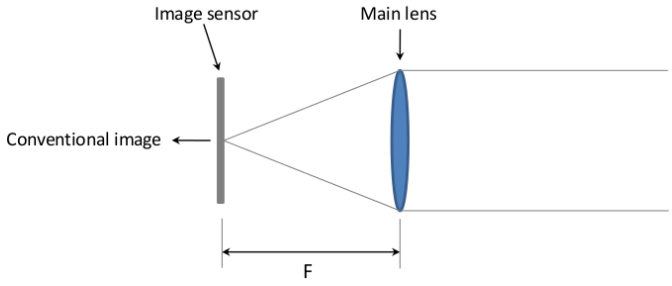

(a) Conventional camera, focused at optical infinity

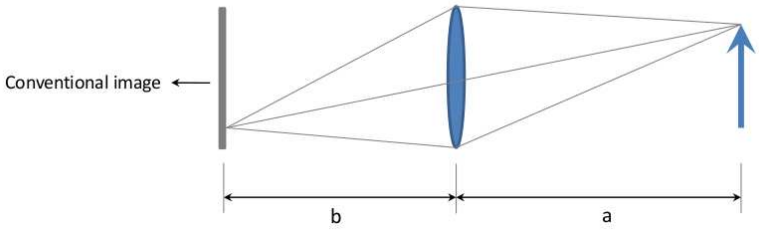

(b) Conventional camera, focused at distance a

Figure 2.1: The abstract representation of a conventional camera setup (a) Focused at optical infinity (b) Focused at distance a

$$\frac{1}{a} + \frac{1}{b} = \frac{1}{F}, \tag{2.7}$$

where a is the distance from the object to the main lens optical centre, b is the image distance to the optical centre of the main lens and F is the focal length of the main lens.

In contrast, plenoptic cameras prevent the averaging of the radiance by introducing spatio-angular selectivity by using a lens array. This method replaces camera arrays with a single camera and an array of small lenses for small baselines. The operating principle behind this light field acquisition method is simple. By placing a sensor behind an array of small lenses or lenslets, each lenslet records a different perspective of the scene, which can be observed from that specific view point on the array. The acquisition method in plenoptic cameras will generate a light field with a (u, v) resolution equal to the number of lenslets and an (s, t) resolution depending on the number of pixels behind each lenslet. Based on this operating principle, different arrangements have been introduced for a plenoptic camera by varying the distance between the lenslet array and the image sensor as well as by adding a main lens to the object side of the lenslet array.

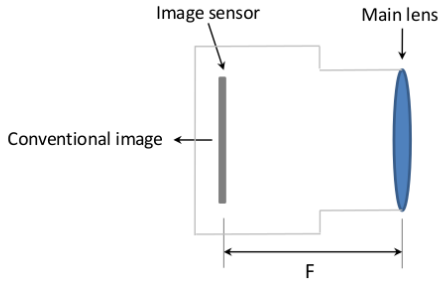

(a) Conventional camera, main lens focused at the optical infinity

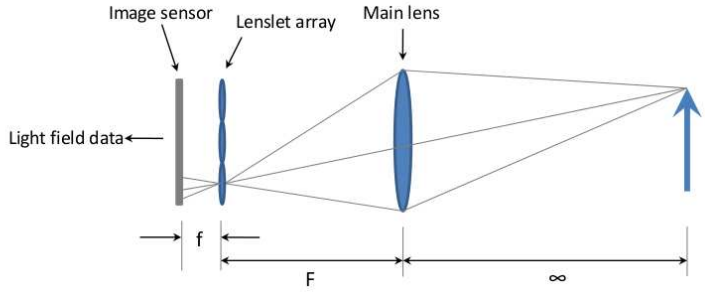

(b) Basic plenoptic camera model, object placed at the optical infinity

Figure 2.2: Basic plenoptic camera versus conventional camera setup (a) Conventional camera, main lens focused at the optical infinity (b) Basic plenoptic camera, main lens focused at the optical infinity

2.5.1 Basic plenoptic camera

The basic configuration of the plenoptic camera (called PC-i hereafter), places the lenslet array at the main lens's image plane [44, 45]. Figure 2.2 illustrates the PC-i structure including the objective lens with focal length F, the lenslet array with the focal length f positioned at the image plane of the main lens, and the image sensor placed at distance f behind the lenslet array. For abetter comparison, the structure of the conventional camera and the basic plenoptic camera are illustrated respectively in Figures 2.2(a) and 2.2(b). The size of each lens in the lenslet array, in some implementations, is of the order of a few tens to a few hundred micro meters and so the lenslet array is sometimes also called the micro lens array. The basic idea behind the PC-i optical arrangement is that the rays that in the conventional camera setup come together in a single pixel, essentially pass through the lenslet array in the PC-i setup, and are then recorded by different pixels (see Figure 2.2(b)). Using this method, each microlens measures not just the total amount of light deposited at that location, but how much light arrives along each ray.

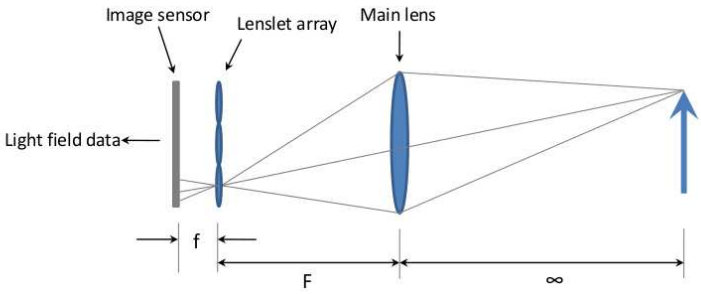

(a) Basic plenoptic camera, main lens focused at the optical infinity

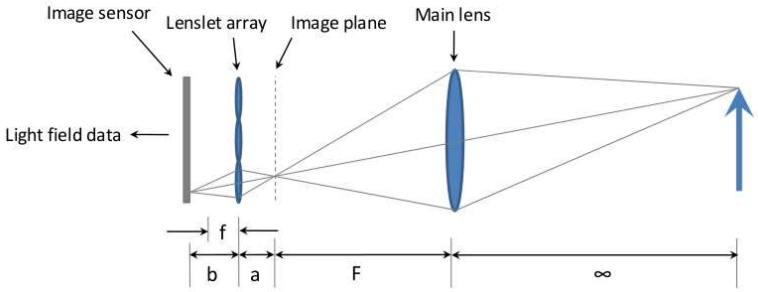

(b) focused plenoptic camera, main lens focused at the optical infinity

Figure 2.3: Focused plenoptic camera versus basic plenoptic camera setup (a) Basic plenoptic camera, main lens focused at the optical infinity (b) focused plenoptic camera, main lens focused at the optical infinity

2.5.2 Focused plenoptic camera

In the second proposed configuration for the plenoptic camera (called PC-f hereafter), the lenslet array is focused at the image plane of the main lens [46, 47]. This configuration is also known as the focused plenoptic camera. For easier comparison, both PC-i and PC-f structures are illustrated in Figure 2.3(a) and 2.3(b) respectively. Figure 2.3(b) provides the details about the PC-f configuration in relation to the fact that the spacing between the main lens, the lenslet array and the image sensor are different to that of the basic plenoptic camera model (Figure 2.3(a)). These variations also cause a different set of camera properties for the PC-f as compared to the PC-i.

In the PC-f configuration, the image plane of the main lens, the lenslet array and the image sensor form a relay system:

$$\frac{1}{a} + \frac{1}{b} = \frac{1}{f} \tag{2.8}$$

where a is the distance from the main lens image plane to the lenslet's optical centre, b is the image distance to the optical centre of the lenslet and f is the focal length of the lenslet.

As can be observed in Figures 2.1 through 2.3, the camera thickness is increasing, from the conventional camera to the PC-i and eventually the PC-f configurations. The increasing camera thickness has brought challenges in applications in which the functionality of the plenoptic cameras are beneficial but their physical size (mainly the thickness) is a serious limitation.

2.6 Camera trade-offs

It was stated that the spatial multiplexing enables there to be a light field capture of dynamic scenes but it requires a trade-off between the spatial and angular sampling rates [21]. Plenoptic cameras, as spatial multiplexing capturing systems, employ the same spatio-angular trade-off. In general, there is a strong inter-relation between the properties in a plenoptic capture such as the viewing angle, different aspects of image resolution and the depth range [48]. To assist in this trade-off process, a characteristic equation has been proposed by Min et al. [49] as:

$$R_s^2 \Delta z \cdot \tan(\frac{\alpha}{2}) = R, \tag{2.9}$$

where R_s is the spatial resolution at the image plane, Δz is the depth range in which objects are accurately reconstructed, α is the lenslet viewing angle and R is the resolution of the image sensor. The point extracted from Equation 2.9 is that there is only a single method by which all the properties can be improved without sacrificing any other, namely, increasing the resolution of the image sensor. All other approaches will merely emphasize one property at the expense of the others [48].

The work of [9] is a good example that attempts to analyze the camera trade-offs in various computational imaging approaches. They show that all cameras can be analytically modelled by a linear mapping of light rays to sensor elements. Thus they interpret the sensor measurements as a Bayesian inference problem of inverting the ray mapping. The work in [9] is elaborating on the existing trade-offs and emphasizes the necessity of a unified means to analyze the trade-offs between the unconventional camera designs used in computational imaging.

However, there are still three remaining major points to discuss for a certain plenoptic capturing system:

- If the image capturing system is making the most of its capabilities for the desired range of applications,
- If the properties of the existing plenoptic capturing system are extracted thoroughly, and
- If the image reconstruction algorithms are making the most of the captured data.

The above discussion topics are basically related to the evaluation of the image capturing system, which is a complex issue in the case of plenoptic cameras

as strongly inter-related systems. A unified framework, which is the main concern of this thesis work, allows us to better understand the light sampling properties for each camera configuration. This framework allows us to investigate the trade-offs between different camera properties, and to analyze their potentials and limitations.

2.7 Chapter summary

This chapter provided the material including the background and terminology to be used in the remainder of this thesis work. Optical models with different complexity levels were presented. There was a discussion regarding the suitability of each optical model for a range of applications and provided different levels in explaining the light behaviour interacting with an optical system. The plenoptic function was then introduced, followed by the concept of the light field as the vocabulary of computational imaging. Two configurations of the plenoptic camera were briefly described and the inevitable trade-offs between camera parameters in various unconventional camera configurations were mentioned. The camera trade-offs section noted that there is a strong inter-relation between the properties of plenoptic capturing systems. This chapter covered:

- The basic terminologies
- The plenoptic capture as a way of slicing (sampling) the 4D light field
- The lack of (or a desire for) a unified system to describe camera properties in general and plenoptic camera properties in particular

Chapter 3

The SPC Model

The SPC framework was initially introduced in Chapter 1 as a framework for the representation and evaluation of plenoptic capturing systems. Inside the SPC framework, the SPC model exists as the main module or the heart of the SPC framework (illustrated in Figure 1.3). This chapter will investigate the SPC model, how it is defined, how it is generated, and will discuss some properties of the SPC model.

3.1 Introduction

The SPC model is a geometrical optics based model that, contrary to the previously proposed ray-based models, includes focus information and this is conducted in a much simpler manner than is the case for the wave optics model. The SPC model carries ray information as well as the focal properties of the capturing system it models. Focus information is a vital feature for inferring high-level properties such as lateral resolution in different depth planes. In relation to carrying the focal properties of the capturing system, the SPC model uses light samples in the form of a light cone (LC).

We consider the light intensity captured in each image sensor pixel in the form of a light cone, the fundamental data form upon which our model is built. Then the SPC model of the capturing system describes where within the scene this data set originates from. This description is given in the form of light cones' spatial position and angular span. The set of spatial positions and the angular spans will form the SPC model of the image capturing system. This knowledge reveals how the light field is sampled by the capturing system. The explicit knowledge concerning the exact origin of each light field sample makes the model a tool capable of observing and investigating the light field sampling behaviour of a plenoptic camera system.

In the following representations, the work is within the (**x,y,z**) space considering **z** as the depth dimension. All the optical axes are supposed to be in parallel with the **z** axis. Projections of the LCs and apertures are supposed to have rectangular shapes with their edges in parallel with **x** and **y** axes. In this case only the geometry

is considered. No content or value is as yet assigned to the model elements.

3.2 Light cone

Previously proposed single light ray based models are parameterized using either a position and direction in 3D space, or a two plane representation. In contrast, the SPC model works with the light sample in the form of the light cone (LC) with an infinitesimal tip and finite base. The LCs represent the form of in-focus light.

A light cone is here defined as the bundle of light rays passing through the tip of the cone represented by a 3D point $(x_c,\, y_c,\, z_c)$, within a certain span of angles $[\phi_s, \phi_f]$ in the **x** direction and $[\theta_s, \theta_f]$ in the **y** direction. Angles are defined relative to the normal of the plane $\mathbf{z}_c$ in the positive direction, where $\mathbf{z}_c = \{(x, y, z) : z = z_c\}$. The angle pairs (ϕ_s, ϕ_f) and (θ_s, θ_f) are always in an ascending order which means $\phi_s \leq \phi_f$ and $\theta_s \leq \theta_f$. If an operation applied to an LC generates a new LC, then the angle pairs for the resulting LC are also sorted to follow this order.

The following notation is utilized for a light cone, using the notation of $r(x, y, z, \phi, \theta)$ as a single light ray passing through (x, y, z) with the angles of ϕ and θ relative to the normal of plane **z** in the **x** and **y** directions:

$$C(x_c, y_c, z_c, \phi_s, \phi_f, \theta_s, \theta_f) = \{\forall r(x_c, y_c, z_c, \phi, \theta) : \phi \in [\phi_s, \phi_f] \wedge \theta \in [\theta_s, \theta_f])\}\,. \quad (3.1)$$

A light cone is hence uniquely defined by its tip location and the angular span. The radiance contained in a light cone is obtained by integrating all light rays within that light cone:

$$\begin{aligned} I(x_c, y_c, z_c) &= \int\int C(x_c, y_c, z_c, \phi_s, \phi_f, \theta_s, \theta_f) d\theta d\phi \\ &= \int_{\phi_s}^{\phi_f} \int_{\theta_s}^{\theta_f} r((x_c, y_c, z_c), \phi, \theta) d\theta d\phi. \end{aligned} \quad (3.2)$$

Theoretically, the base of a light cone can have any polygon shape but, in this case, only a rectangular base shape is used for simple analysis and illustration purposes. This assumption will not affect the generality of the concept and is compatible with the majority of the existing plenoptic camera arrangements. The notation can be adjusted to other base shapes if required.

3.3 The sampling pattern cube

The sampling pattern cube (SPC) is a set of light cones C_i:

$$SPC := \{C_i\}\,, i = 1, \ldots, k. \quad (3.3)$$

The SPC is defined as a set and thus there can be a discussion in relation to superimposing two (or more) SPCs, here shown by $'+'$, as the union operation applied to these two (or more) SPCs:

$$SPC_1 + SPC_2 := \{C_i\} \cup \{C_j\}\,, \quad (3.4)$$

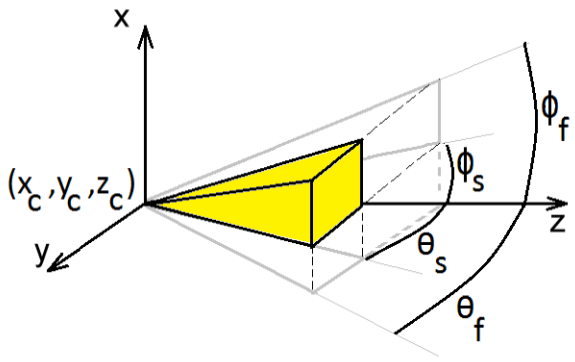

Figure 3.1: Illustration of a light cone in three dimensional space

where

$$SPC_1 := \{C_i\}, i = 1, \ldots, k$$
$$SPC_2 := \{C_j\}, j = 1, \ldots, r$$

The LCs in the SPC model carry the information about the position within the scene that the light field samples come from. The SPC thus gives a mapping between the pixel content captured by the image sensor and the 3D space outside the image capturing system. To simplify further descriptions of the model, as well as illustrations of the same, we henceforth reduce the dimensionality by ignoring the parameters relating to the y-plane. Figure 3.2 illustrates a light cone in 2D space which is parameterized as:

$$C(x_c, z_c, \phi_s, \phi_f). \tag{3.5}$$

Expanding the model to its full dimensionality is straightforward. Ignoring the parameters relating to the y-plane, the first dimension of the SPC is the location of the light cone tip x, relative to the optical axis of the capturing system. The second dimension is the light cone tip's depth z along the optical axis, relative to the reference plane $\mathbf{z}_0$ and the third dimension is the angular span of the light cone ϕ. The reference plane $\mathbf{z}_0$ can be arbitrarily chosen to be located at the image sensor plane, the main lens plane, or any other parallel plane as long as it is explicitly defined. Although an axial symmetry of the optical system is assumed in this description, the approach can be easily extended to a non-symmetrical system.

The choice of using light cones renders a more straightforward handling of in-focus light ray information compared to previously proposed two-plane and point-angle representations [11, 12, 28] and is unique for a determined optical system. Two capturing systems will sample the light field stemming from the scene in the same way if their SPCs are the same.

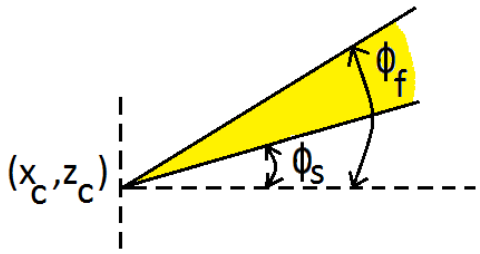

Figure 3.2: Illustration of a light cone in 2D space

3.4 Operators

At this point a number of operators applied to single light cones as the fundamental elements of the SPC model are defined. Operators are applied to an LC and generate parameters, a new LC, a set of LCs or an emptyset. Operations can also be applied to a set of LCs. If an operator is used, which produces a new LC in its output, then the operation affects all the single LCs in the set and hence generates a new set of LCs.

3.4.1 Base operation

Base or boundary $B[\cdot]$ of the light cone C on the plane $z = z_0$ (that is the intersection area of that LC with the depth plane $z = z_0$) is illustrated in Figure 3.3, and is defined as:

$$B\left[C, z_0\right] := (x_1, x_2, z_0, \phi_1, \phi_2) \tag{3.6}$$

where

$$\begin{aligned} x_1 &= x_C + (z_C - z_0)\tan\phi_s, \\ x_2 &= x_C + (z_C - z_0)\tan\phi_f, \\ \phi_1 &= \phi_s, \\ \phi_2 &= \phi_f. \end{aligned}$$

The Base operator is a one to one mapping between the light cone and the parameters it generates as the output. So the reverse operation exists and is shown as:

$$C = B^{-1}\left[x_1, x_2, z_0, \phi_1, \phi_2\right], \tag{3.7}$$

where

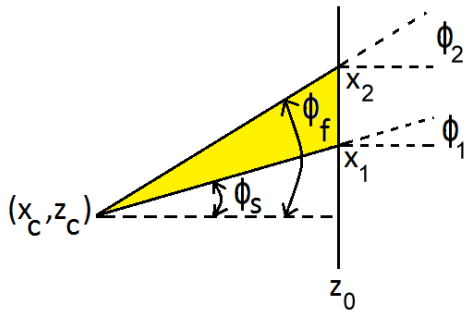

Figure 3.3: Base or boundary of a light cone on the plane $z = z_0$

$$
\begin{aligned}
z_c &= \tfrac{x_2 - x_1}{\tan\phi_2 - \tan\phi_1} + z_0, \\
x_c &= \tfrac{x_1 \tan\phi_2 - x_2 \tan\phi_1}{\tan\phi_2 - \tan\phi_1}, \\
\phi_s &= \phi_1, \\
\phi_f &= \phi_2.
\end{aligned}
$$

3.4.2 Translation operation

A Translation operation $T[\cdot]$ is applied to a given LC and translates the tip position of the LC by the given amount (x_T, z_T), not affecting the angular span of the LC:

$$T\left[C, x_T, z_T\right] := C'(x_{c\prime}, z_{c\prime}, \phi_1, \phi_2) \tag{3.8}$$

where

$$
\begin{aligned}
x_{c\prime} &= x_c + x_T, \\
z_{c\prime} &= z_c + z_T, \\
\phi_1 &= \phi_s, \\
\phi_2 &= \phi_f.
\end{aligned}
$$

3.4.3 Aperture operation

An aperture operation $A[\cdot]$, where the aperture parameters such as aperture plane $z = z_A$, starting position x_{1A} and the ending position x_{2A} of the aperture are known, is applied on the LC in the following manner:

$$A\left[C, x_{1A}, x_{2A}, z_A\right] := \begin{cases} \emptyset & if\ \ [x_{1A}, x_{2A}] \cap [x_1, x_2] = \emptyset \\ C' & if\ \ [x_{1A}, x_{2A}] \cap [x_1, x_2] = [x_1', x_2'], \\ C & if\ \ [x_{1A}, x_{2A}] \cap [x_1, x_2] = [x_1, x_2] \end{cases} \tag{3.9}$$

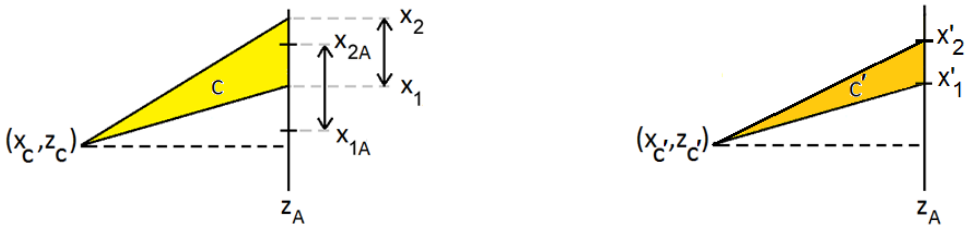

(a) (b)

Figure 3.4: Aperture operation applied to a single light cone (a) Initial light cone (b) Resulted light cone

where

$$C' = B^{-1}\left[x'_1, x'_2, z_A \arctan\frac{x'_1}{z_A - z_C}, \arctan\frac{x'_2}{z_A - z_C}\right],$$

and x_1, x_2 are derived from applying the $B[\cdot]$ operation to the light cone:

$$B\left[C, z_A\right] := (x_1, x_2, z_A, \phi_1, \phi_2)\,.$$

Figure 3.4 represents how a light cone is affected by applying the aperture operator.

3.4.4 Lens operation

The lens operation imitates the geometrical optics properties of an ideal lens. A lens operation $L[\cdot]$ is applied to a light cone and provides a new light cone. The lens parameters such as the lens plane $z = z_L$, position of the lens optical axis x_L, the focal length of the lens f and the hyperfocal distance d_L for the lens are known in this operation. In the case where the results of a lens operation are parallel light rays, they are treated as a cone with their tip position at the plane of the hyperfocal distance from the lens, which means if the resulting LC is considered as C', then: $z_{C'} := d_L$

The lens operation considers the lens to be infinitely wide and it affects an LC in the following manner:

$$L\left[C, x_L, z_L, f\right] := \begin{cases} C' & if\ f > 0 \\ C & if\ f = \pm\infty \\ C'' & if\ f < 0 \end{cases} \tag{3.10}$$

and

$$C' = B^{-1}\left[x_1, x_2, z_L, \phi_s - \arctan\left(\frac{x_1 - x_L}{\frac{f(z_L - z_C)}{(z_L - z_C) - f}}\right), \phi_f - \arctan\left(\frac{x_2 - x_L}{\frac{f(z_L - z_C)}{(z_L - z_C) - f}}\right)\right],$$

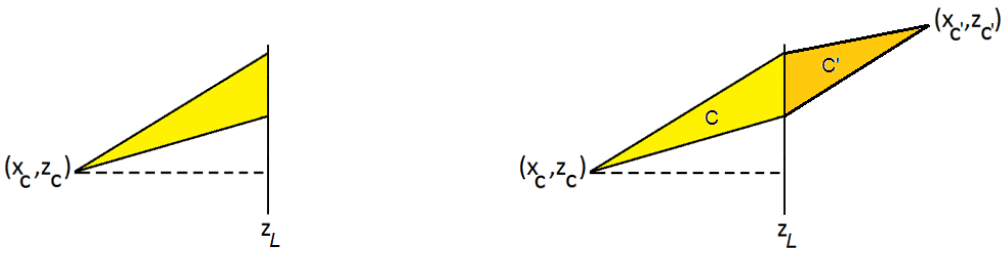

(a) (b)

Figure 3.5: Lens operation applied to a single light cone (a) The initial light cone (b) The initial and the resulted light cone

$$C'' = B^{-1}\left[x_1, x_2, z_L, \phi_s + \arctan\left(\frac{x_1 - x_L}{\frac{f(z_L - z_C)}{(z_L - z_C) - f}}\right), \phi_f + \arctan\left(\frac{x_2 - x_L}{\frac{f(z_L - z_C)}{(z_L - z_C) - f}}\right)\right],$$

where x_1 and x_2 are obtained from the $B[\cdot]$ operation applied to the light cone:

$$B\left[C, z_L\right] := (x_1, x_2, z_L, \phi_1, \phi_2)$$

Equation 3.10 uses the lens equation to find the new tip position and angular span of the resulting light cone from the lens operation. Figure 3.5 represents how the lens operation is applied to an exemplary light cone in the case of a lens with $f > 0$ and $z_L > z_C$.

3.4.5 Split operation

The split operation $S[\cdot]$ takes an LC and a set of split parameters as the input and generates a set of new LCs. Split parameters are the split plane $z = z_S$, starting positions x_{sk} and the ending position x_{fk} of the k^{th} split sections. Here are the constraints for the split sections:

- The split sections should not overlap
- The split sections should cover the whole range of $[x_1, x_2]$ where x_1 and x_2 are obtained from:

$$B\left[C, z_S\right] := (x_1, x_2, z_S, \phi_1, \phi_2) \tag{3.11}$$

The split operation $S[\cdot]$ works in the following manner:

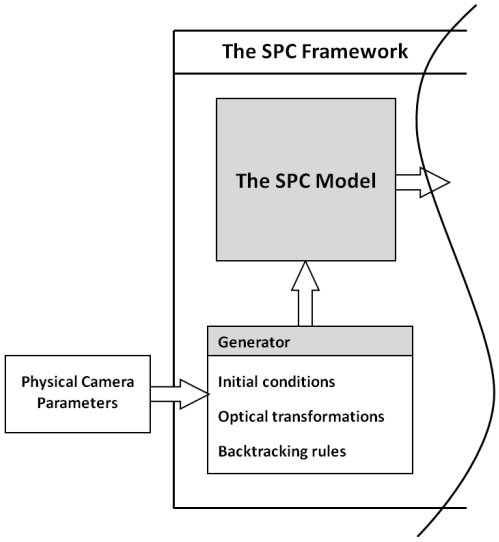

Figure 3.6: The SPC model generator module

$$S\left[C, x_{s1}, \ldots, x_{sk}, x_{f1}, \ldots, x_{fk}, z_S\right] := \left\{C'_1, \ldots, C'_k\right\}, \tag{3.12}$$

where

$$C'_i = A\left[C, x_{si}, x_{fi}, z_S\right], \quad i = 1, \ldots, k$$

3.5 The SPC model generator

In order for an SPC to carry the information about the light field sampling behaviour of the optical system, it is required to be built in a particular way. The initial set of the light cones must pass through the optical system in order to extract the sampling properties of the optical system. At this point, a description will be given regarding how the SPC model is generated using the physical camera parameters fed to the generator module, the initial conditions, the defined operators in Section 3.4 and the rules which will be described in this section. Part of Figure 1.3, that illustrates the SPC model generator module, is reprinted here in Figure 3.6 for ease of access.

Building the SPC model is based on the following basic assumptions:

- The fundamental light samples captured by an image sensor is a set of light cones
- This set of light cones are back-traceable into the physical 3D capturing space in front of the camera

- The final result of this back-tracing process is a new set of light cones as the SPC model of the capturing system

To generate the SPC model of a capturing system, we start from the initial set of LCs with their tip position at the centre of each pixel on the sensor plane and an angular span equal to the light acceptance angle of each sensor pixel. Then we back-track each LC through the optical system, passing elements such as apertures and lenses, which will transform the initial set of LCs into new sets using geometrical optics. The transformations continue until we reach a final set of LCs with new tip positions and angular spans that carry the sampling properties of the capturing system. This final set of LCs and their correspondence to the initial sensor pixels, build the SPC model of the system and preserve the focal information and the information regarding where each recorded light sample on the sensor cell is originating from.

The current way of producing the initial set of LCs with one LC per pixel could be extended to an arbitrary number of LCs per pixel without any loss of generality. Two types of extensions to the single LC per pixel scenario are presented in Section 4.2.3.

To expand the above description concerning the SPC model generating process, two implementation approaches are considered. One starts from the initial set of the light cones and back-traces all of them to the next stage by applying a suitable operator (called, here, the operator-based approach). The second implementation takes only one light cone related to one pixel, and back-traces that single light cone all the way into the captured scene in front of the camera system and then goes to the next light cone related to the next pixel. This second approach will be called the pixel-based approach.

These two approaches are implementation-wise slightly different. However, if the full SPC model of the camera system is desired, the two approaches provide the same final results. If a partial SPC model of the camera system is preferred, either of the above implementation approaches can be computationally more efficient depending on the optical structure of the camera. The partial SPC model is the SPC model of not the whole capturing system, but only a part of it. In periodic structures (such as a plenoptic capturing setup) it is computationally beneficial to generate the partial SPC model of the system, corresponding to the image sensor and one single lenslet, and construct the full SPC model of the capturing system by means of a proper translation (see Section 3.4.2) and by superimposing (see Equation 3.4) the partial SPC models.

3.5.1 Operator-based approach

Consider the first set of light cones having their tip locations positioned at the image sensor pixel locations, and their angular span defined by the light acceptance angle of the sensor. Thus we have an initial set of light cones, named S_i, for which the tip position and angular span of the cones are derived from the physical camera parameters, namely the image pixel pitch and the light acceptance angle of each pixel on

the image sensor. The next step towards generating the SPC model of the capturing system is to back-trace this initial set of light cones into the scene. A combination of optical transformations act on the light cones as a consequence of back-tracing the set of light cones through the optical system. These transformations are applied to all the LCs using the defined operators in Section 3.4.

In a plenoptic capturing setup (as described in Chapter 2 and Figure 2.3), the first operation applied to this initial set of light cones is the aperture operation, since, starting from the image sensor side and following the optical path towards the space in front of the camera, the first optical element to reach to is the lenslet array. In order to apply the aperture operator, $A[\cdot]$, to the light cones, required parameters such as the aperture plane, $z = z_A$ are derived from the physical camera parameters fed to the model generator module. Other required information is the starting position x_{1A} and the ending position x_{2A} related to the geometry of the lenslet system. For each lenslet in the lenslet array, the aperture operator is defined and applied to S_i. If the pixels behind a lenslet are optically decoupled from those behind any neighbouring lenslets, then the aperture operation related to a single lenslet is only applied to those LCs which belong to the pixels behind that specific lenslet. The resulting set of light cones, after applying the lenslet's aperture, S_a will then be the input of the next optical transformation.

Now that the initial set of light cones, S_i, are trimed into the new set, S_a by using the aperture operator, the next optical transformation is applied, which is the lens effect regarding the lenslet array in the plenoptic camera structure. For each lenslet in the lenslet array, the lens operator, $L[\cdot]$, is defined and applied to S_a. Parameters required for defining the lens operator, which include the lens plane $z = z_L$, position of the lens optical axis x_L and the focal length of the lens f are again extracted from the physical camera parameters fed to the model generator module. The output of this stage is a set of light cones S_{la} which is the union set of all the outputs from single lenslets. The light cones in S_{la} will then be the input of the next optical transformation.

Following the optical path towards the space in front of the camera, the next optical element which will be met is the main lens (camera objective), and so the next operation applied to the current set of light cones, S_{la} is the aperture operator associated with the main lens. Required parameters for this operator are the aperture plane and the starting position and the ending position related to the geometry of the main lens. applying the aperture operator to S_{la} will provide us with the new set of LCs, here called S_{ala}. The final optical transformation is the lens effect associated with the main lens where the main lens optical axis and the focal length of the main lens F are obtained from the list of physical camera parameters.

When no more optical transformations remain to be applied to the LCs, the process of generating the SPC model is over. The final set of light cones, located outside the image capturing system but within the captured scene forms the SPC model.

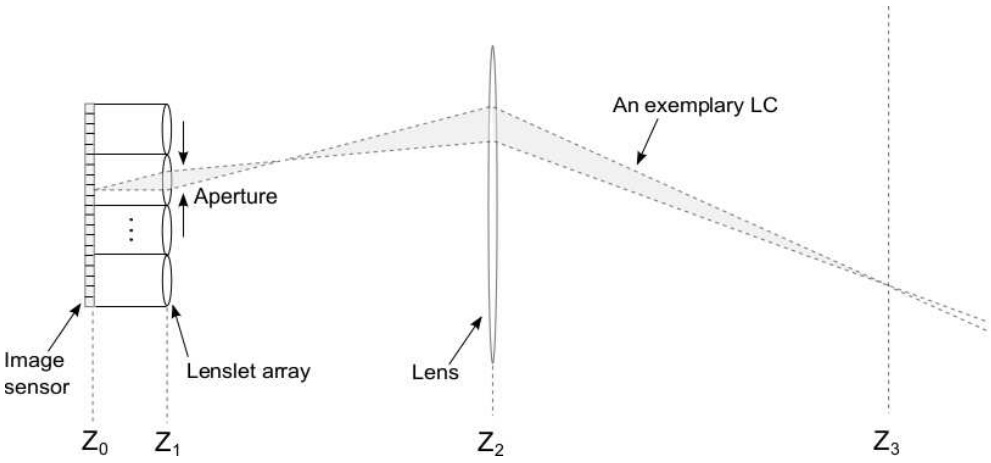

Figure 3.7: Illustrating the process of backtracking an exemplary LC into the space in front of a camera

3.5.2 Pixel-based approach

A general description is now provided regarding how the SPC model of the capturing system is generated using the pixel-based approach. For each pixel in the image sensor, repeat until no more optical elements are to be considered:

1. Define the initial light cone associated with that pixel according to the pixel position and the light acceptance angle of that pixel.
2. Define the operation that should be applied to that light cone considering the camera configuration in the back-tracing process.
3. Apply the operation and generate the new LC.

The SPC model of the capturing system is then the union set including all the processed LCs located outside the image capturing system but within the captured scene.

Figure 3.7 shows the process of back-tracing an exemplary LC into the space in front of an exemplary plenoptic camera (with PC-f configuration). The figure demonstrates how the LCs are backtracked from the sensor plane, $z = Z_0$, passing the lenslet array at plane $z = Z_1$ and the main lens at plane $z = Z_2$ and reaching into the space in front of the camera (back in-focus at plane $z = Z_3$).

3.6 Chapter summary

The SPC model was introduced in this chapter together with the SPC model generator module. It was stated that:

- The SPC model is distinct from the previously proposed models by using the light samples in the form of the light cones (LCs).
- The SPC model includes focus information of the capturing system carried by the LCs.
- The focus information of the capturing system is vital for inferring high-level properties of the capturing system.
- Light field sampling properties of the capturing system are reflected in the SPC model of the capturing system. The SPC model carries the information specifying angular and spatial positions from which the captured information by each pixel in the camera sensor originates. This knowledge is scene independent and provides the necessary information about the sampling behaviour of the image capturing system.

The contribution of the author to this chapter:

- Introducing the SPC model that describes the light sampling properties of a plenoptic capturing system and the instructions and rules for building the SPC model.

Chapter 4

The SPC Model Visualization

The SPC model has been described in Chapter 3 as a model that reflects the light field sampling behaviour of the plenoptic capturing system. This chapter will investigate how the SPC model is visualized and also how to benefit from the visualization module for a better understanding of the light field sampling behaviour of the plenoptic capturing systems. Figure 4.1 regenerates part of Figure 1.3 related to the visualization module. The output of the the visualization module, graphically represents the LCs that build the SPC model of the camera.

4.1 Introduction

As described in Chapter 3, the SPC model uses light samples in the form of light cones (LCs).

The explicit knowledge about the exact origin of each light field sample makes the model a tool capable of observing and investigating the light field sampling behaviour of a plenoptic camera system. The light field sample captured by each image sensor pixel is in the form of a light cone, the fundamental data form that our model is built upon. In the SPC model of the capturing system, it is defined where within the scene this data set originates from. This description is given in the form of light cones' spatial position and angular span. The set of spatial positions and the angular spans will form the SPC model of the image capturing system. This knowledge reveals how the light field is sampled by the capturing system.

In the following representations, the work is within the (**x,y,z**) space considering **z** as the depth dimension. All the optical axes are supposed to be in parallel with the **z** axis. The work only deals with the geometry and no content or value is yet assigned to the model elements.

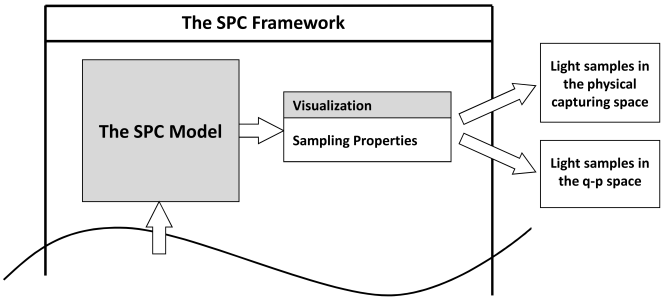

Figure 4.1: The visualization module in the SPC framework

4.2 Visualizing the light samples in the SPC model

We use the data captured by the camera as an estimate of the original light field. The sampling properties of the capturing device forms one source of the deviation of the capatured data from the original light field. Noise, lens chromatic aberrations, imperfections and implementation tolerances are other contributors which are not discussed here. If we consider the image pixel size being the maximum precision of a point, we arrive at a sampled space of the light field using the proposed SPC model.

4.2.1 Representing the light cones in the 3D capturing space

The first approach visualizes each light cone by representing a physically truncated cone inside the physical capturing space in front of the camera. The geometry of the cone tip and its angular span is given by the corresponding light cone it represents. Visualizing the SPC model, which is a set of light cones, will result in a set of physically truncated cones with their tips located inside the 3D capturing space in front of the camera. If we consider the LCs in their full dimensionality, this visualization approach will result in a 3D space containing 3D light cones. The tip positions and the span of the visualized light cones indicate how the camera samples the light field in the capturing space. The name ”sampling pattern cube” originates from this approach for visualizing the light field samples in the 3D capturing space in front of the camera. An exemplary result for visualizing a number of light cones using this approach is shown in Figure 4.2.

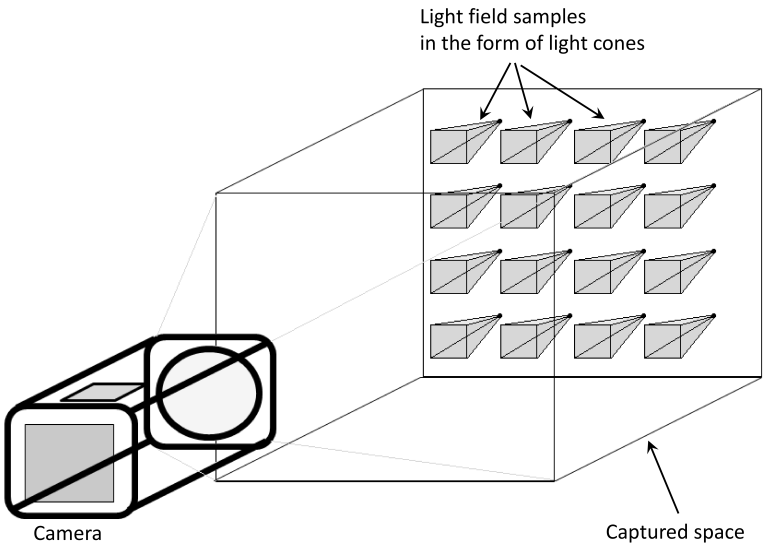

Figure 4.2: Visualizing light cones in the capturing space

4.2.2 Representing the light cones in the q-p space

Before investigating the **q**-**p** space representation of the light samples in the SPC model, there will be a brief discussion regarding the **q**-**p** space representation of the ray optics which will be used later as a handy notation in the investigation of the SPC model light field sampling properties. More about the **q**-**p** space representation and application of the ray-based optics can be found in [50, 51].

In the two dimensional notation, a single ray passing the point $(x, z = 0)$ with angle ϕ relative to the optical axis **z**, can be represented by a point as (x, ϕ) on the (q, p) plane, where **q** is the position axis and **p** is the angle axis (see Figure 4.3(a)). A single light cone, which is recalled as a bundle of all rays passing the tip position of the cone with a particular angle spread, in the **q**-**p** notation is then represented as a vertical line segment (see Figure 4.3(b)).

In a furtur extension, all the light cones with their tip positions between $(x = x_1, z = 0)$ and $(x = x_2, z = 0)$ and sharing the same aperture on plane $z = z_A$ will be represented in the **q**-**p** plane as a tetrahedral patch with two vertical edges (see Figure 4.3(c)).

If the x values are not continuous but are limited to a set of discrete values (e.g. due to the image sensor's finite pixel size), then the **q**-**p** representation of a set of distinct light cones with their tip position between $(x = x_1, z = 0)$ and $(x = x_2, z = 0)$, and sharing the same aperture on plane $z = z_A$ will be limited to a vertical grid

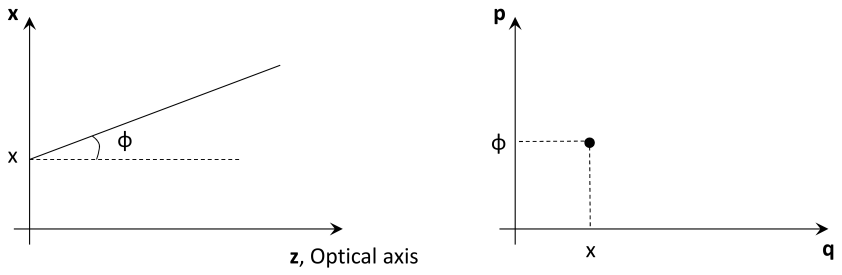

(a)

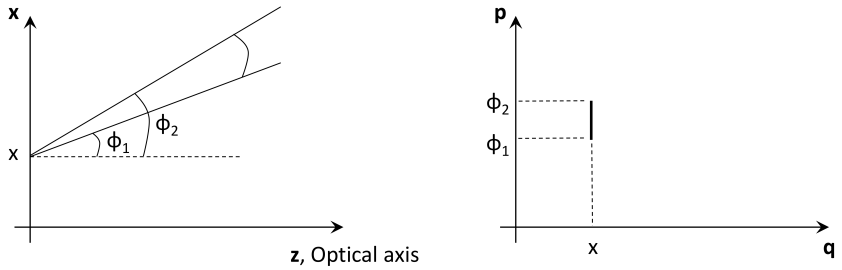

(b)

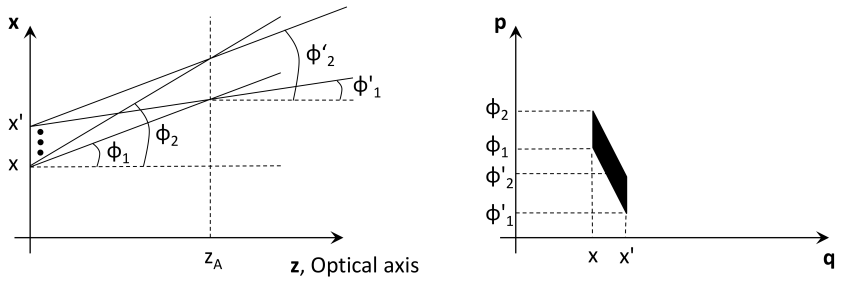

(c)

Figure 4.3: x-z versus q-p representations for (a) A single ray (b) A single LC (c) A continiuous range of light cones with their tip positions covering the range between $(x = x_1, z = 0)$ and $(x = x_2, z = 0)$ and sharing the same aperture on plane $z = z_A$

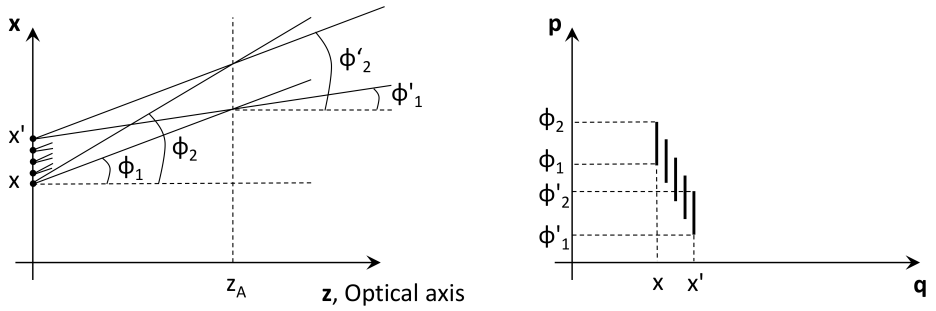

Figure 4.4: x-z versus q-p representations with discrete x positions

in the (q, p) plane (see Figure 4.4).

Since there is a one to one mappings between all the rays crossing the **x** axis and the points in the (q, p) plane, the transformations between the (x, z) and (q, p) planes are all reversible. As a result, for example, a vertical line segment in the **q**-**p** space is the representation of a light cone with the tip position located on the **x** axis in the (x, z) plane.

4.2.3 The SPC model in the q-p space

The **q**-**p** space representation of the SPC model of a plenoptic capturing system assists to envision the light field sampling behaviour of the capturing system. The key point in this step is how to relate the initial light cones to each pixel on the image sensor plane, so that it is possible to later interpret the SPC model of the capturing system in line with our initial assumption. Three scenarios are considered here which cause marginal differences in interpreting the light field sampling properties of the SPC model. These three scenarios respectively assume that:

I The initial LCs' peaks are located at the centre of each pixel (see Figure 4.5(a))

II The initial LCs' peaks are located behind each pixel with the spread equal to the pixel size (see Figure 4.5(b))

III The initial LCs' peaks are located at the start and end point of each pixel (see Figure 4.5(c))

Assuming LCs' peaks to be located at the centre of each pixel (case I) is the simplest (both in terms of implementation and model complexity) and is the scenario that has been utilized in the SPC model generator (Section 3.5). It assumes that all the rays coming to each pixel are collected by the centre point of the pixel, which is a fair approximation for certain applications.

The two other scenarios (cases II and III) offer a more accurate interpretation of the light field sampling behaviour of the capturing system but at the same time add

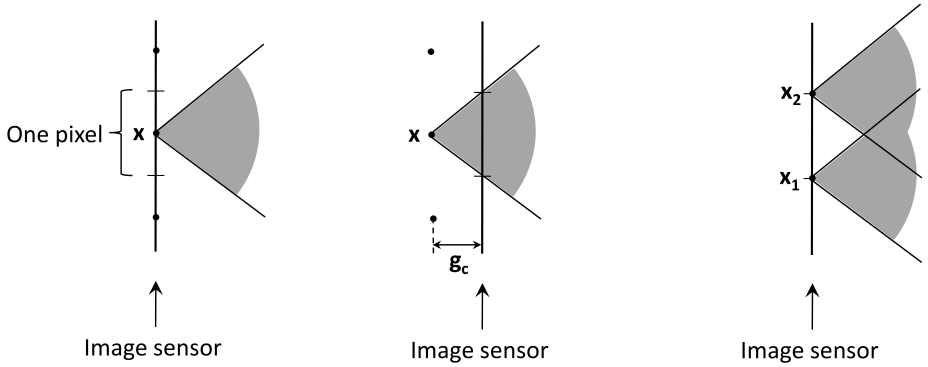

(a) (b) (c)

Figure 4.5: Three scenarios for assigning LC(s) to an image sensor pixel (a) Peak position of the LC is located at the pixel's centre point (b) Peak position of the LC is located behind the pixel with the spread equal to the pixel size (c) Peak position of the LCs are located at the start and end point of the pixel

to the complexity of the SPC model. However, both cases II and III can be reverted to the first scenario (case I). In case II, a virtual shift back of the image sensor plane in the **z** direction with the amount equal to g_c will bring the case II back to the case I. It means that we can then use the same SPC model generator (previously defined for the first scenario) but with the new geometry. To revert case III back to case I, a virtual shift of the image sensor this time in the **x** direction by an amount equal to half of the pixel pitch will cause this to occur.

From the modelling accuracy point of view, assuming LCs being located at the start and end point of each pixel (case III) provides a more accurate interpretation of the light field sampling behaviour of the capturing system. An even more accurate assumption is to consider the whole range of the LCs with their tip positions located on the span of a single image sensor pixel to contribute to the radiance captured by that image sensor pixel. In this case, each pixel is sampling a patch in the (q, p) plane (as previously shown in Figure 4.3(c)) rather than a single line segment (see Figure 4.3(b)).

As the accuracy of the model is increased, the complexity is also growing. It is important to recall that there is only one value assigned to the radiance captured by each image sensor pixel and assigning more than one light cone to each pixel asks for a valid approach to split this single value among several LCs. This might be achievable to some extent, where prior knowledge about the geometry of the scene, the surface properties and the lighting conditions exist.

Table 4.1: Utilized camera parameters in visualization of the SPC model

Parameter	PC-i	PC-f
Main lens focal length, F	$80mm$	
The gap between main lens and lenslet array	$80mm$	$97mm$
Lenslet focal length, f	$1.5mm$	
Lenslet pitch	$0.5mm$	
Lenslet array size	100×100	
The gap between lenslet array and image sensor	$1.5mm$	$1.7mm$
Image sensor pixel size	$6.8\mu m \times 6.8\mu m$	

4.3 Visualising the SPC model in the q-p space for plenoptic capturing systems

In this case, the SPC model visualization is investigated for an exemplary plenoptic capturing system using the **q**-**p** representation. The dimensions of the SPC model are continued to be reduced in the given example in order to simplify the discussion as well as the illustrations.

A few examples are provided in [52], showing how the SPC model is applied to the optical capturing systems, and how the variations in the geometrical parameters of the system are reflected in the SPC model visualization of the system. The utilized notation in [52] switches the position, **q** and angle, **p** dimensions to retain the vertical axis being reserved for the position of the LCs' tips, in both **x**-**z** and **q**-**p** representations. What is shown in this section is according to the **q**-**p** representation's notation given in Section 4.2.2, and so the LCs are presented by vertical line segments.

From the two configurations of a plenoptic camera (discussed in Section 2.5), the first configuration or PC-i, places the lenslet array at the main lens image plane. In the second configuration or PC-f, the lenslet array is focused at the image plane of the main lens (focused plenoptic camera)[46]. Different optical arrangements in these two camera configurations cause significant differences in their light field sampling properties. The distinction between their light field sampling properties is also reflected in their respective SPC models and can be observed and investigated using the visualization module in the SPC framework.

In either PC-i or PC-f configurations, by assuming the same focal length for all of the lenslets, the SPC model of the plenoptic capturing system will include a set of LCs with their tip positions located in a single depth plane and thus this is sufficient to visualize the content of that single depth plane in order to visualize the whole SPC model of the capturing system.

As the first step, the SPC model is generated for the two PC-i and PC-f configurations using the parameters summarized in Table 4.1. For later comparison purposes, parameters of the main lens and the lenslets array are considered to be the same in both configurations and the main lens is focused at the optical infinity.

The SPC model of the exemplary PC-i and PC-f configurations are visualized in

Figures 4.6 and 4.7 using the **q**-**p** space notation. For clarity, only a subset of the full SPC is presented, corresponding to a single row of pixels behind a single row of the lenslets. It is still the case that the number of visualized LCs is large (about 73×100) and so they cannot all be seen individually. Thus an inset is magnifying a small portion of the (q, p) plane to be investigated. The two insets in Figures 4.6 and 4.7 have the same scale for easier comparison and values are excluded in order to maintain the generality of the cases.

The overall shape of the sampled area, in the SPC model of the PC-i and the PC-f configurations, specify that the distributions of the light samples (LCs) are quite different in these two capturing arrangements.

In the SPC model of the PC-i configuration, the depth plane where the final LCs' tip positions are located is placed at distance F (focal length of the main lens) from the main objective outside the camera. In this configuration, the main lens is focused at the optical infinity. Examining the SPC model of the PC-i configuration visualized in Figure 4.6, light cones from the pixels behind a single lenslet have an angular span which smoothly shifts from one LC to the other (the highlighted row in the inset) and light cones from the pixels behind the adjacent lenslets share the tip position and add to that angular span. This sampling behaviour provides multiple angular samples for one single spatial position in that specific depth plane. This behavior results in a parallelogram shape as the sampled area in the SPC model of a PC-i configuration (see Figure 4.6).

In the PC-f configuration, the plane containing the LCs' tip positions is located at the hyper focal distance of the main lens. Examining the SPC model of the PC-f in Figure 4.7, light cones from adjacent lenslets do not share their tip location. Instead, the light samples from a single lenslet, compared to those from the adjacent lenslet, are shifted in the positional as well as the angular dimensions. In this case, each light cone adds to the number of individual light cone tip positions in the SPC model which will thus provide a bigger number of resolvable positional data. Observing the visualized SPC model associated with the PC-f configuration (Figure 4.7), the number of the angular samples associated with one spatial position is limited due to the constant shift of the light cones from the pixels behind one lenslet. This behavior results in a shape similar to a thick line as the sampled area in the SPC model of a PC-f structure (see Figure 4.7).

Variations in the capturing system are reflected in the SPC model of the capturing system. As an example, if we add to the number of lenslets in the PC-i and PC-f structures (and at the same time expanding the size of the image sensor with the same pixel density to support the larger area covered by the lenslet array), we observe different outcomes in the corresponding SPC models. In the SPC model of the PC-i structure, for each added lenslet, one row of LCs is added to the top (or bottom) of the parallelogram (see Figure 4.6), thus making it cover a bigger angular range (a longer parallelogram) without a change in the number of positional samples (the parallelogram retains the same width). It means that adding lenslets in the PC-i structure increases the number of angular samples per positional values, but not the number of the positional samples.

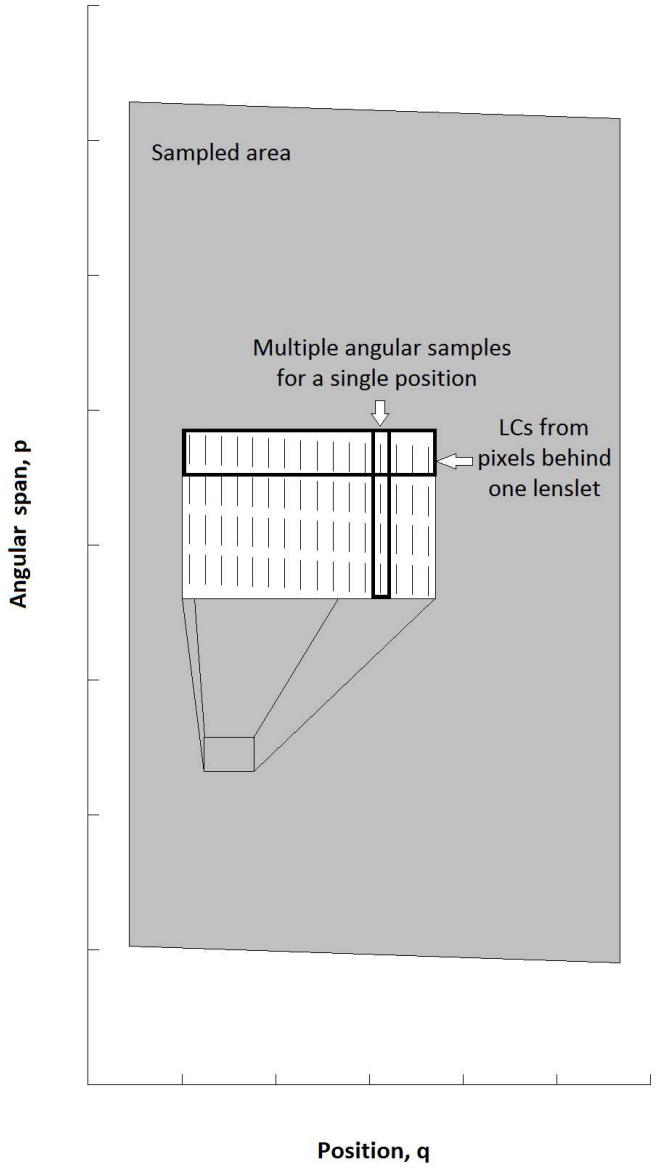

Figure 4.6: The **q**-**p** space visualization of the SPC model of an exemplary plenoptic camera with PC-i configuration

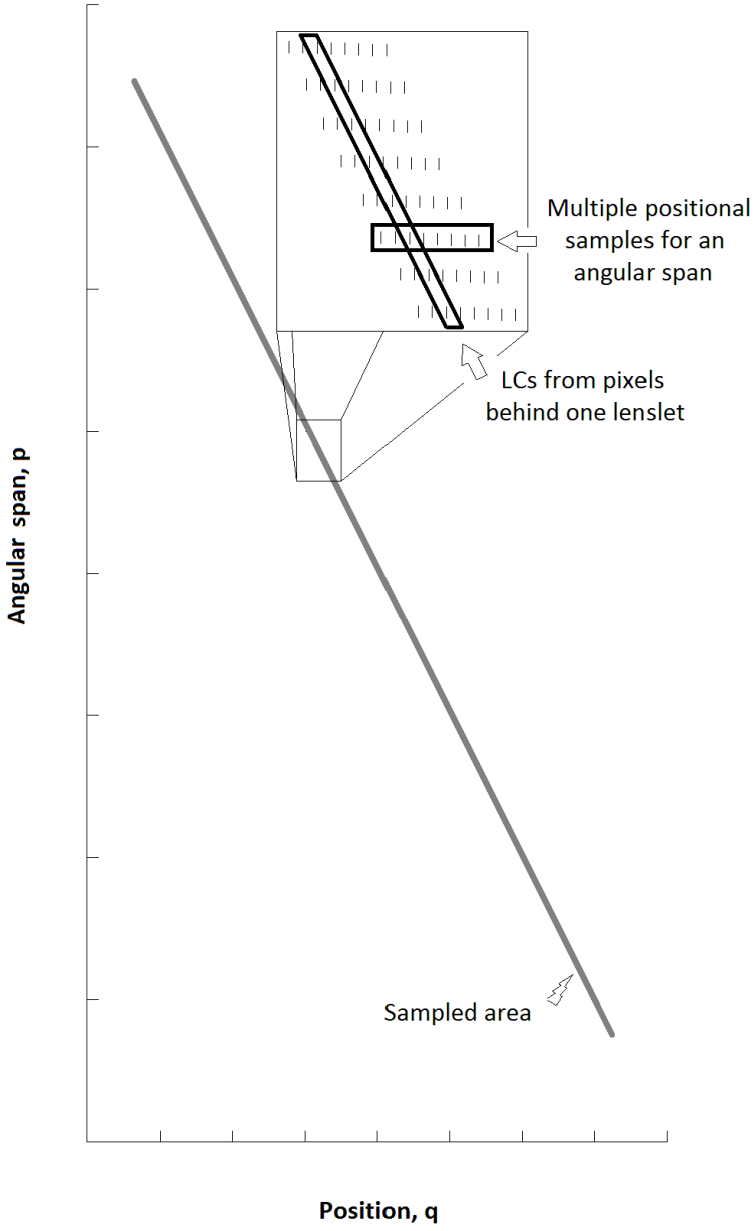

Figure 4.7: The **q**−**p** plane visualization of the SPC model of an exemplary plenoptic camera with PC-f configuration

The case is different in the PC-f structure. Adding lenslets in the PC-f structure increases the number of different positional samples in the SPC model of the camera system, represented as a longer thick line in Figure 4.7. However, it does not affect the angular range (or the thickness of the thick line marked as the sampled area in Figure 4.7).

4.4 Benefiting from the SPC visualization

The SPC provides the information about where in the captured space, the light information recorded in each pixel is originating from. Based on this interpretation of the SPC model, the LCs can be visualized in the captured space. Visualization in the (x, z) coordinate as well as the (q, p) plane were previously discussed in Section 4.2. Visualization can provide a better insight into the light field sampling behaviour of the capturing system, and so assist us in different applications ranging from the design of new capturing system arrangements to developing better image reconstruction algorithms. Dynamic visualisation of the SPC variations in the case of a plenoptic camera setup with varying parameters can also be enlightening for educational purposes.

4.5 Chapter summary

Since the SPC model is incorporating the light samples in the LC form which is the in focus light samples, the **q**-**p** representation of the SPC model includes only vertical line segments for the plenoptic camera configurations. For the PC-i and PC-f camera configurations, the SPC model was visualized using a single (q, p) depth plane. The SPC model visualization can include more than a single (q, p) plane in the plenoptic camera configurations, which, for example, use multi focus lenslet systems.

As the SPC model represents the light field sampling properties of the capturing system, visualizing the SPC model assists in a better understanding of the sampling properties. Using methods for visualizing the SPC model, we can explore how the system variations are revealed in the SPC model based representation of the capturing system.

The contribution of the author to this chapter:

- Introducing the visualization module in the SPC framework
- Describing the 3D capturing space representation of the LCs
- Describing the **q**-**p** space representation of the LCs
- Discussing how we can benefit from visualization of the SPC model

Chapter 5

The SPC Property Extractors

This chapter presents how the important high-level properties such as lateral resolution are extracted from the SPC model which was represented in Chapter 3. Property extractors are major components in the evaluation module (see Figure 5.1) inside the SPC framework. In Figure 5.1, a set of property extractors has been described as independent parts of the evaluation module inside the SFC framework. Each property extractor has access to the SPC model of the capturing system as the input of the evaluation module and will extract a high-level property of the capturing system.

Some of the high-level properties of the plenoptic capturing systems and how they are reflected in the SPC model are qualitatively investigated in [52] as a publication resulting from this thesis research work. However, the concept of the feature extractors in the SPC model, and more specifically, a property extractor to quantitatively extract the lateral resolution property in a plenoptic capturing system is initially introduced in [53]. The main focus in this chapter is on the lateral resolution as an interesting high level property in a plenoptic capturing system.

5.1 Lateral resolution property extractor

Resolution in plenoptic cameras is an example that demands more detailed investigations, which gives consideration to the properties of the capturing system. Such investigations of complex capturing system have been the subject of prior and recent works [8, 10, 54]. In this chapter, there is a description regarding how to extract lateral resolution from the SPC model and in Chapter 6, the lateral resolution extractor is validated with respect to results from wave optics based Monte Carlo simulations and practical measurements.

Lateral resolution for a complex plenoptic capturing system is defined as the inverse of the minimum distance between two resolvable points located at a specific depth plane within the system's common field of view (CFV). Depending on the purpose of the lateral resolution analysis, the number and locations of depth planes

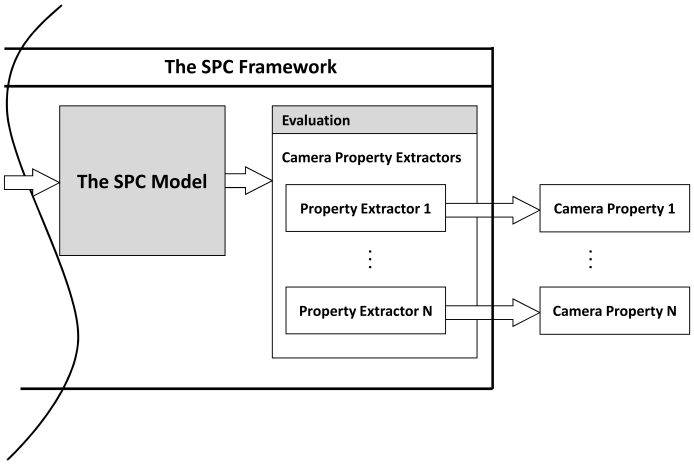

Figure 5.1: The evaluation module inside the SPC framework

may be arbitrarily chosen. The captured resolution in a plenoptic camera can vary for different depth planes or different distances from the main optical axis.

The property extractors presented here are built based on the idea that the lateral resolution in the SPC model can be defined as a function of the light cone distribution and span in each depth plane. To extract lateral resolution using the SPC model we need to apply proper adjustments to the general definition and incorporate the specific features of the model.

Three approaches are implemented in this case, based on three different definitions of the lateral resolution in a SPC model. All the proposed property extractors extract the lateral resolution from the SPC model throughout an arbitrary number of depth planes resulting in a depth-resolution profile. These property extractors utilize information embedded in the elements of the SPC model, including the focal properties of the capturing system and the geometrical distribution of the light cones.

5.1.1 First lateral resolution property extractor

The first property extractor defines the inverse of the lateral resolution value (the lateral resolution limit, Res_lim) as the maximum Euclidean distance, d_e between immediate neighbouring LCs' base centre points:

$$Res\_lim = \text{Max}(d_e). \tag{5.1}$$

Figure 5.2 shows an example of neighbouring LCs and their respective base area and centre point. Two LCs are immediate neighbours if no other LC's base centre point is located between their base centre points. In this first definition, no focal

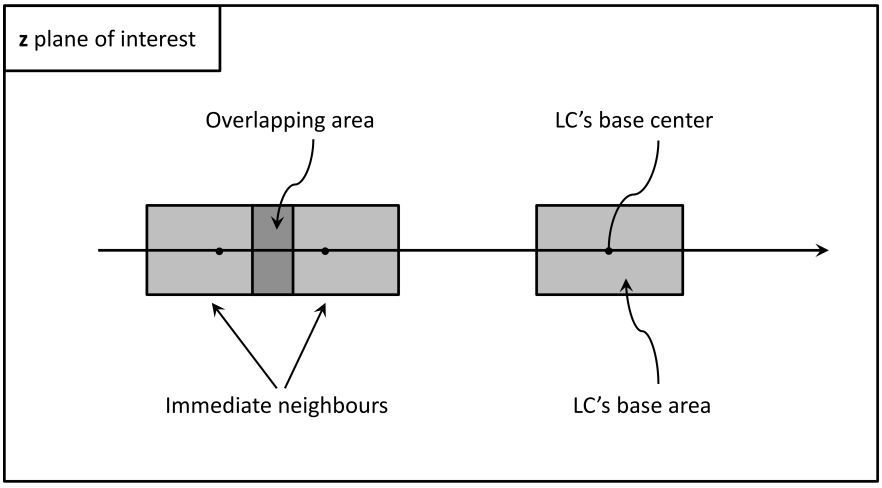

Figure 5.2: Illustration of the LC's base area and centre point

property is used, and the lateral resolution extractor reduces the SPC model to a ray model as only the principal rays passing through the LCs' centres are used to investigate the capturing system properties.

5.1.2 Second lateral resolution property extractor

The second and more elaborate lateral resolution property extractor utilizes the SPC model's focal information, which is preserved as the width, w of the LCs at each depth plane:

$$w = x_2 - x_1, \tag{5.2}$$

where x_1 and x_2 are obtained from Equation 3.6 as the boundaries of the light cone's base area at the desired depth plane $z = z_0$. The second lateral resolution property extractor considers the freedom of movement of a point inside an LC's base area. The inverse of the lateral resolution value at a certain depth plane is defined as the largest of the following values: 1) maximum Euclidean distance, d_e between centre points of two immediate neighbour LCs, or 2) half of the maximum LC's base width, w at that depth plane:

$$Res\_lim = \text{Max}(d_e, \frac{w}{2}), \tag{5.3}$$

where Res_lim is the inverse of the lateral resolution (the lateral resolution limit).

The following assumptions are made to cause the proposed measure reflect the actual resolution:

- The resolution test points can only be located where the system is able to sample them, which means inside the LCs in the SPC model (a consequence of the sparse sampling model).
- Two points are resolvable only if they are located within two different LCs.
- Two LCs are considered different if they do not include the centre of each other
- The distance between two LCs is defined as the Euclidean distance between their centre points, d_e.

To find d_e valid for the whole CFV, the worst case is sought, i.e. we consider the two immediate neighbour LCs that have the maximum distance from each other. Then either of the following cases holds:

Case 1 If these two immediate neighbour LCs are not overlapping, then Res_lim is equal to d_e.

Case 2 If these two immediate neighbour LCs are overlapping but they are still different LCs, then the Res_lim is equal to the d_e.

Case 3 If these two immediate neighbour LCs are overlapping and they include the centres of the other, then all the LCs in the SPC are overlapping and the Res_lim is equal to the half of the LC's width.

The process to find Res_lim value is presented in Figure 5.3 where the two illustrated base areas belong to the two immediate neighbour LCs with the maximum distance between their centre points.

5.1.3 Third lateral resolution property extractor

To investigate more thoroughly the characteristic of the SPC model in extracting the lateral resolution, the previous lateral resolution extractor is modified and a new extractor with improved functionality is buit. The pixel size projected in each depth plane is an attribute, which is included in the third definition for the lateral resolution feature extractor. How this modification affects the accuracy of the results will be discussed in Chapter 6. It should be noted that the projected pixel size at a certain depth plane is also a part of the system properties embedded in the SPC model in the form of the distance between two initially neighbouring LCs at the depth plane of interest.

In this third lateral resolution extractor, the concept of resolvability is applied where at least one LC (pixel) exists which contains one of the point light sources but not the other. This means that there should be a light cone, which is not contributing to the content of the first pixel, but does to the second. Following the above definition, the lateral resolution extractor in the SPC model which extracts the lateral resolution limit, Res_lim in a certain depth plane is described as:

$$Res\_lim = pps + min\_dist \tag{5.4}$$

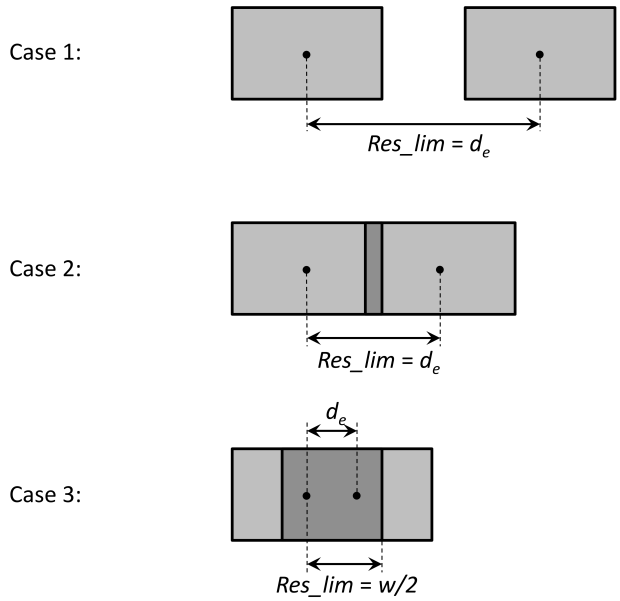

Figure 5.3: Finding the resolution limit in the second lateral resolution property extractor

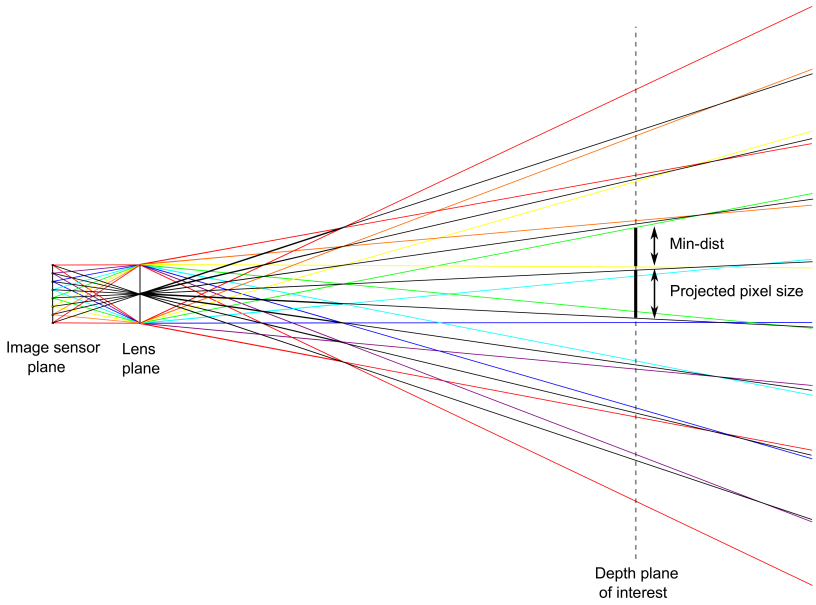

Figure 5.4: Illustrating the contributors in the lateral resolution limit on the depth plane of interest (third definition)

where pps is the projected pixel size in the depth plane of interest and min_dist is the length of the maximum line piece created by the overlapping span of the LCs in that depth plane (see a single lens example in Figure 5.4).

5.2 Chapter summary

Being able to readily quantify the high level properties of a capturing system is of practical use for conventional image capturing systems in general, but of specific interest when working with more complex systems such as camera arrays [55] and light field or plenoptic cameras [56].

The contribution of the author to this chapter:

- Introducing the evaluation module in the SPC framework
- Defining three lateral resolution property extractors

Three lateral resolution property extractors have been introduced that incrementally leverage on the SPC features: the centre of the bases of the LCs at each depth plane, the width of bases of the LCs at each depth plane, the distribution of the LCs at each depth plane and finally the projected pixel size at each depth plane. All the parameters used by these property extractors are provided by the SPC model of the capturing system.

Chapter 6

Evaluation of the SPC Framework

In this chapter the descriptive level of the SPC model is evaluated by investigating the capability of the model in describing the high level properties of the capturing system. The SPC framework including the model generator, the SPC model and the evaluation modules are implemented in Matlab for a set of exemplary plenoptic capturing systems.

6.1 Methodology

To evaluate the SPC framework, the previously defined property extractors are applied to a set of exemplary plenoptic capturing system setups. The property extractors are evaluated by comparing the results to those from the ray based model and the wave optics based Monte Carlo simulations for the same capturing systems. The validity of the wave optics based Monte Carlo simulations results is confirmed by physical experiments [10, 54, 57] and so this data is considered as the ground-truth of the evaluated system in terms of lateral resolution. In a further step, how variations in the plenoptic capturing system (for example in the image sensor pixel size) influences the final extracted property are investigated and whether the results fall in line with those from the more elaborated models.

6.2 Test setup

Two plenoptic capturing systems have been considered for the evaluation of the proposed lateral resolution extractors. The pixels behind each lenslet are assumed to be optically decoupled from any neighbouring lenslets in all the test setups. Figure 6.1 illustrates the considered setup for the evaluation of the proposed lateral resolution

Table 6.1: Test setup specifications

Parameter	Setup 1	Setup 2
Lenslet array size	11×11	11×11
Lenslet focal length, f	$12mm$	$12mm$
Lenslet pitch	$4.2mm$	$4.2mm$
Lenslet f-number, f/D	22	22
Spacing between lenslet array and image sensor, g	$12.507mm$	$12.507mm$
Image sensor pixel number behind one lenslet	251×251	301×301

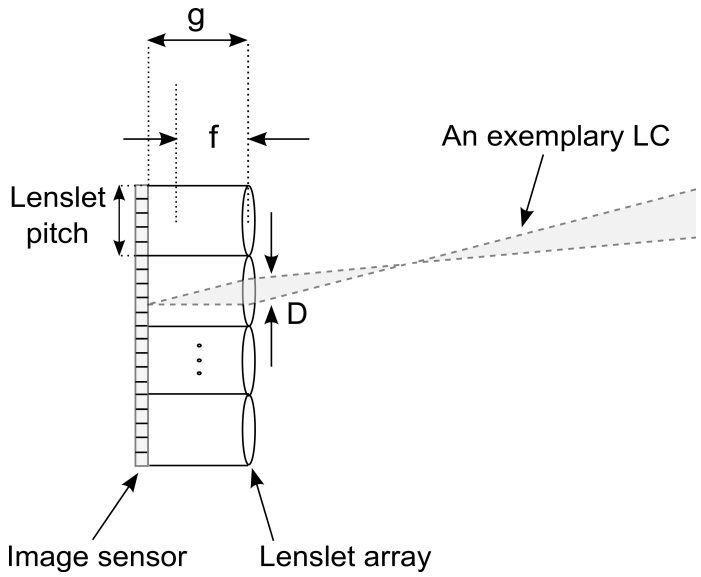

Figure 6.1: Illustration of the test setup utilized in the evaluation of the lateral resolution property extractors

extractors and the specifications of the test setups are given in Table 6.1.

6.3 Results and discussion

In this part, the results from the three lateral resolution property extractors are provided. The results are compared to those from the ray based model and the wave optics based Monte Carlo simulations for the same capturing systems.

6.3.1 The first lateral resolution property extractor

The first lateral resolution extractor (as defined in Section 5.1) considers only the distances between the centre of the LCs, which is equivalent to the position of the

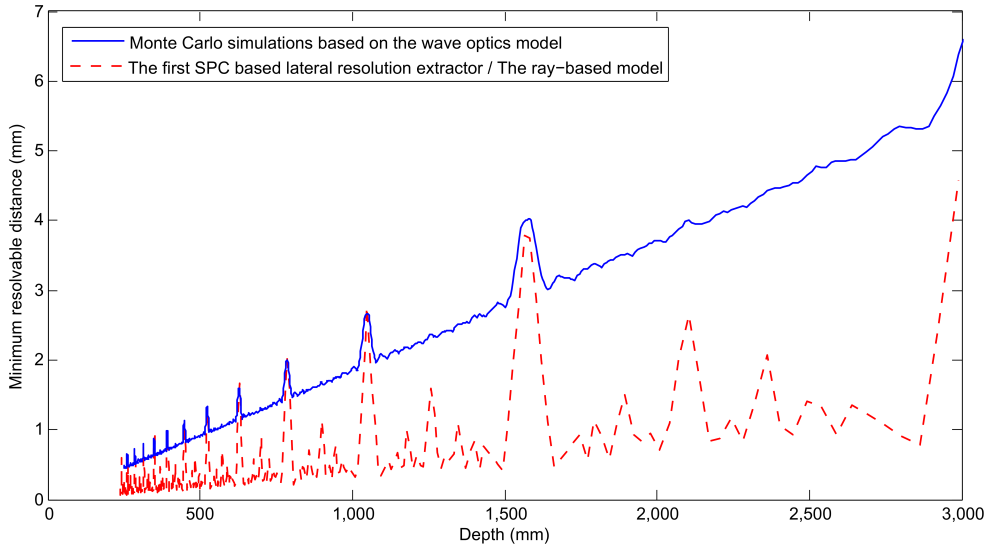

Figure 6.2: The minimum resolvable lateral distance at different depth planes achieved from the first proposed lateral resolution extractor (equal to the results when using only the principal rays), and the reference data from wave optics based Monte Carlo simulations

principal rays, in extracting the lateral resolution of the plenoptic system under investigation. This first extractor ignores the focal properties of the capturing system, which are presented in the form of the LCs span in each depth plane. Thus, the results from the first lateral resolution extractor are basically equal to what can be expected from a ray tracing model based on the principal rays.

The first lateral resolution property extractor is applied to the SPC model of the plenoptic capturing system stated as Setup 1 in Table 6.1 and the results for the lateral resolution extracted using this first extractor are shown in Figure 6.2. The results are shown together with those from the wave optics based Monte Carlo simulations as reference data for comparison purposes. The focal plane of the system in Setup 1 is about 300 mm and the data at depth planes further away than this are presented. A correction factor of two is also applied to the result from the SPC-based extractor relative to the wave optics based data. This takes into consideration the difference between the two methods, for which the former extracts resolvability using dark-light points and the later dark-light-dark points.

A general trend is observed in both graphs shown in Figure 6.2 which indicates that there are depth planes where the lateral resolution drops (location of peaks on the minimum resolvable distance graphs) compared to depth planes slightly closer or further away. This resolution drops can be explained using the distribution of the LCs or, in this case, the distribution of the centre points of the LCs' bases. In the resolution dropping depth planes, LCs overlap and form clusters and the lateral resolution is decreased as a result of the poorer distribution of the LCs.

It is observed, that the results from the lateral resolution property extractor equal to the ray-based model, which is using only the distance of the LCs' centres, can set only an upper limit on the lateral resolution in different depth planes. We can call this value the upper limit of the resolution since it is assuming the ideal case where all the information is carried by the centre of the LC (or the single ray).

Results from the first extractor are aligned with the wave optics based Monte Carlo simulations results in terms of the location of the peaks and periodicity of the depth planes with low-resolution (the peaks in the graphs shown in Figure 6.2). However, the general slant of the results from the first extractor and values at the intermediate depth planes do not match with the results from the wave optics based Monte Carlo simulations.

Noting that the SPC model allows for the production of results equal to a ray-based model, makes that ray based model a subset of the SPC model. In another words, if the lenslet array is reduced to a pinhole array, the SPC model is reduced to the ray-based model where the rays are actually the LCs with an infinitely small span of the cone.

6.3.2 The second lateral resolution property extractor

The second lateral resolution extractor (as defined in Section 5.1) incorporates the focal properties of the plenoptic capturing system in the form of the span or width of the LCs in the process of extracting the lateral resolution property of the plenoptic capturing system. This second extractor is applied to the same plenoptic capturing setup (Setup 1 in Table 6.1) and the results are shown in Figure 6.3 together with the reference results from the wave optics based Monte Carlo simulations.

We can see in Figure 6.3 that, by using the second lateral resolution extractor, the gap between the upper limit of the resolution (from the first lateral resolution extractor) and its amount from the wave optics based Monte Carlo simulations is considerably reduced. The second lateral resolution extractor is using the distribution of the centre point of the LCs bases (as the principal ray information stored in the SPC model) and the width of the LCs (as the focal property of the capturing system). The resolution values from the second lateral resolution extractor prove to fall better in line with the Monte Carlo simulations data. Graphs agree in location of peaks, maximum amplitudes as well as the general slant at the intermediate depth planes. A gap still exists between the results from the second lateral resolution extractor, which considers more of the SPC properties and the ground-truth reference data.

6.3.3 The third lateral resolution property extractor

The third proposed feature extractor (as defined in Section 5.1) provides the lateral resolution as a function of the projected pixel size, the span of the LCs and their distribution at each depth plane. All contributors to the proposed lateral resolution

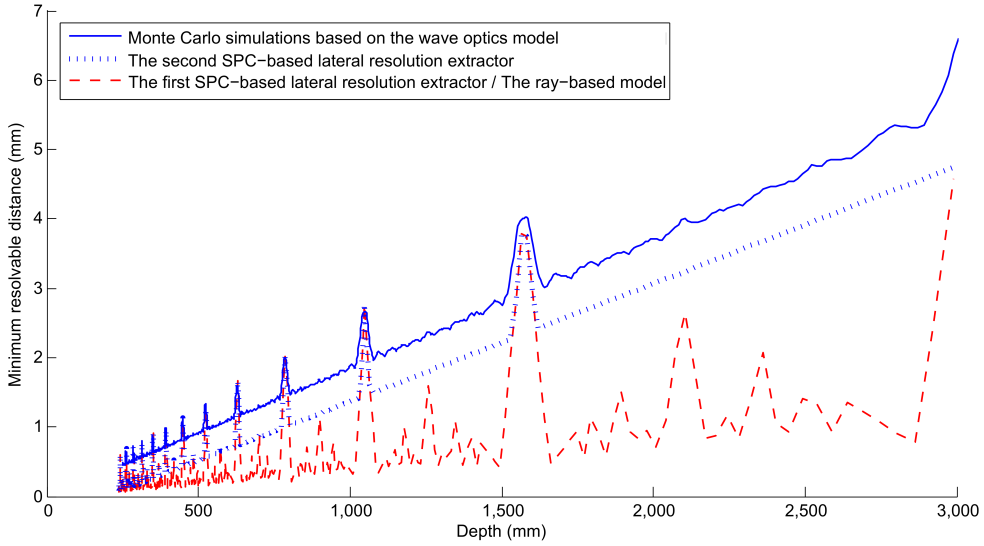

Figure 6.3: The minimum resolvable lateral distance at different depth planes achieved from the second proposed lateral resolution extractor and the reference data from wave optics based Monte Carlo simulations

property extractor are obtained from the geometry and focal properties of the capturing system which are embedded in the SPC model of the system.

Figure 6.4 shows the minimum resolvable distances, or the inverse of the lateral resolution using the third extractor for a range of depth planes, for Setup 1. The data from the ray-based model as well as the wave optics based Monte Carlo simulation results are also provided as reference data for comparison purposes. The focal plane of the system, which is used as te test setup is about 300 mm and the data at depth planes around and further away than this are also presented. Results from the third proposed lateral resolution extractor prove to fall in line with the Monte Carlo simulation results for the examined range of the system parameters.

6.3.4 Comparison of the results from the three extractors

The first property extractor for lateral resolution is very simple and faster to compute compared to the second and third extractors, although the results from this first extractor only show where the planes of the resolution drop are located and the value of the lateral resolution only at those depth planes fall in line with the reference data. The first lateral resolution extractor has the simplest structure of the three and also the lowest descriptive level.

The second lateral resolution extractor starts to incorporate the LCs width and offers results which agree with the reference data in terms of the position and values of the resolution drop planes and the general slant of the lateral resolution graph.

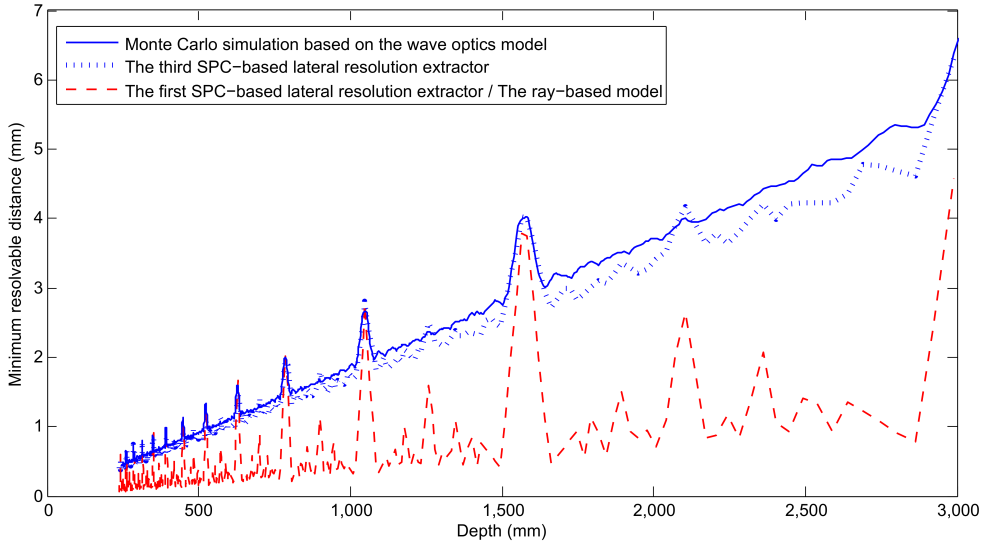

Figure 6.4: The minimum resolvable lateral distance at different depth planes achieved from the ray-based model, the third proposed lateral resolution extractor, and the reference data from wave optics based Monte Carlo simulations

The second lateral resolution extractor adds to the computing work load but does provide results which offer a better agreement.

The third extractor, which includes the projected pixel size, is much more in line with the reference data. This third extractor has the highest computing work load of the three extractors but offers an improved functionality by including the projected pixel size as an influencing factor in the computed lateral resolution value.

6.3.5 Comparison of the results from Setup 1 and 2

Figure 6.5 gives the lateral resolution limit results using the third extractor in the SPC model for both Setups 1 and 2. The graph showing the third lateral resolution extractor results for Setup 2 is also closely in line with the Monte Carlo simulation results (not shown in Figure 6.5) for the respective capturing setup.

The effect of the varying pixel number per lenslet on the lateral resolution limit of the system can be observed in Figure 6.5 mainly as a stretching effect in the z direction. This effect is qualitatively explained by recalling the projected pixel size, pps, and the maximum line piece, min_dist (see Figure 5.4) as the two parameters directly contributing to the lateral resolution limit at the depth plane of interest (for the third SPC-based lateral resolution extractor) and investigating their contributions. The increased pixel number per lenslet results in a smaller pixel size and so a smaller pps for Setup 2 as compared to Setup 1 at the same depth plane is expected. Since the pps is the major contributor to the slant of the minimum resolvable distance graph,

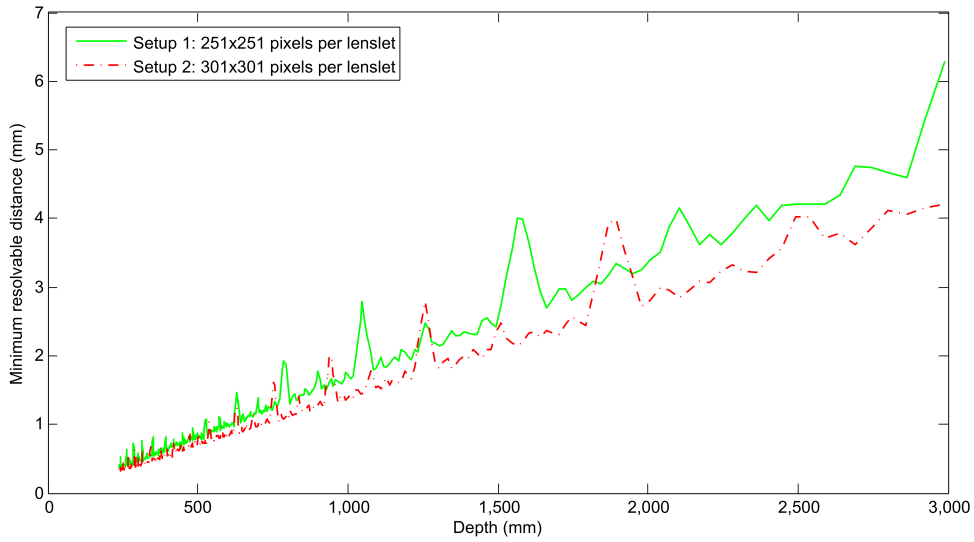

Figure 6.5: The effect of varying pixel density (varying the pixel number over a fixed area) behind each lenslet on the lateral resolution limit using the third lateral resolution extractor

the results corresponding to Setup 2 then have a smaller general slant compared to the results corresponding to Setup 1. Additionally, the width and the distribution of the LCs in the depth plane of interest, illustrated in the parameter min_dist, are major contributors to the location and amplitude of the peaks in the results obtained from the third lateral resolution extractor. The poor distribution of the LCs, which has been called the clustering effect, and which is causing large values for min_dist, generates the peaks in the minimum resolvable distance graphs. Increasing the pixel number per lenslet while maintaining the other parameters constant will cause the clustering of the LCs to occur in proportionally further depth distances and so resulting in a proportional shift in the position of the peaks in the z direction. Results from the third lateral resolution extractor for Setups 1 and 2 demonstrate the SPC lateral resolution extractor as a straightforward predicting tool for investigating the effect of system variations on the lateral resolution limit of the system.

6.4 Model validity

Given in this chapter, the three lateral resolution extractors have been validated by comparing the obtained lateral resolution results with those from the Monte Carlo numerical simulation based on the more elaborate wave optics model. Following this, an investigation has been conducted into how the lateral resolution profile in depth varies with variations in the density of pixels behind each lenslet as an example of the capturing system parameters.

The lateral resolution predicted by the SPC model agrees with the results from wave optics based numerical simulations. Concerning the model's validation method, the comparison to simulated data is considered to be sufficient since the validity of the wave optics based Monte Carlo numerical simulations has been confirmed in [54] and [57] for the same plenoptic capturing system setups.

The lateral resolution extractors in the SPC framework are validated for the case of plenoptic capturing systems. A geometrical feature of these image capturing systems is that they have a periodic structure and hence sample the light field in a periodic pattern. This fact has also been of assistance in relation to the definition of the lateral resolution extractors, which means that a generalization of the property extractors to other capturing systems is applicable only after proper adjustments.

The SPC model can be used for extracting the high level properties of the plenoptic capturing system such as the lateral resolution. The results are valid for the range for which the dominant features are the methods of the geometrical optics. The SPC model fails for those ranges where, for example, the wave nature of light is governing. For example if the SPC model is employed in the design process of a capturing system, the predictions of the model are valid for the range in which the geometrical optics are sufficiently accurate. Other models must be employed to refine predictions of the high level properties of the capturing system from the SPC model at different stages of a design process.

The SPC model fails, for example, to explain or include the aberrations of the main objective lens and the diffraction caused by the f-number of the lens. Higher f-numbers intensify the diffraction effect, at the same time low f-numbers increase the undesirable effect of the lens aberrations. None of these effects are handled by the SPC model and so there is only a middle range of f-numbers for which the SPC model can actually make sufficiently detailed predictions about the plenoptic capturing system using that f-number. Defining the exact limitations and validity ranges of the SPC model requires more future investigations.

6.5 Relating the SPC model to other models

Models previously proposed to describe how the light field is sampled by different image capturing systems range from, simple ray-based geometrical models to complete wave optics simulations, each with a different level of complexity and a varying level of explaining the system's capturing properties. Provided models are easy to work with and accurate in scope, although they hardly provide a unique representation of the sampling behaviour of a capturing system.

Both the ray-based model and the SPC model are defined in the scope of the geometrical optics models, and so the governing method is the same for both of these models (returning to Table 2.1 in Chapter 2). The number of the light elements in the model then becomes a handy figure in order to discuss the computational complexity of the two models. The SPC model assigns a single light cone to each pixel on the image sensor. In the case for which the ray-based model assigns a single

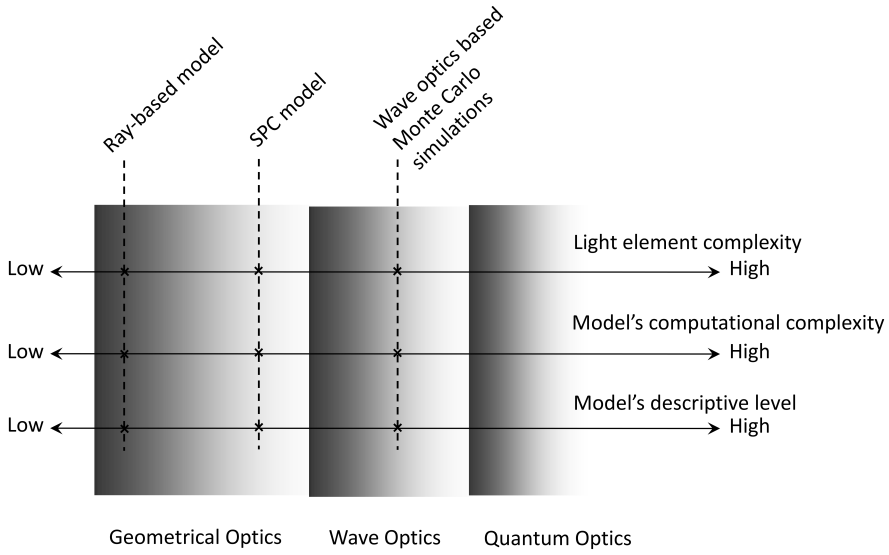

Figure 6.6: A graphical illustration of the complexity and descriptive level of the SPC model compared to other optical models

ray (for example the principal ray) to each image sensor's pixel, the computational complexity of these two models can be considered to be in the same range.

Since the ray-based model is located at the low complexity side of the model complexity spectrum, and the complexity of the SPC model is also in the same range, the SPC model is also placed within the low complexity part of the spectrum. The wave optics and the quantum optics models are placed within the high complexity part of the computational complexity spectrum based on their significantly more elaborate light elements and governing methods. Figure 6.6 places the above description of the model complexity in a graphical representation.

One clear distinction between the SPC model and the ray-based model is the capability of the SPC model in carrying the focal properties of the image capturing system. The information regarding the focal properties of the capturing system is embeded in the angular span of the light cones (or the width of the light cones' base area on arbitrary depth planes). This information is the key in extracting the high level properties of the capturing system (such as lateral resolution) with an acceptable level of details. Considering the capability of the SPC model in carrying the focal properties, provides a higher descriptive level of the system properties to the SPC model as compared to the ray-based model. The descriptive level of the models is graphically represented as the third spectrum in Figure 6.6. Since the SPC model works only within the scope of the geometrical optics, it cannot extract the high level property of the capturing system when the wave optics properties of light are the dominant feature. A good example of such a case is in relation to the effect of lens aberrations and diffraction limitations on the lateral resolution of the capturing

system.

Another distinction between the SPC model and the ray-based model is based on the nature of the light elements in these two models. Light cones as the light samples in the SPC model employ a continuous angular range but discrete positional values. This sampling property is closer to the real physical process that occurs in an image sensor compared to the discrete angular and positional samples being considered in the ray-based model. The continuous range of the angular values in a light cone allows for the spread of radiance information over the base area of the light cone when required. This property might prove to be useful in expanding the model by assigning the radiance values to each light cone (or each image sensor pixel) in the future.

6.6 Chapter summary

In this chapter, an in-depth investigation of the lateral resolution as a high level property of a plenoptic capturing system using the SPC model has been conducted.

It was stated that: The SPC model fills the gap between ray-based models and wave optics based models (or the real system performance), by including the focal information of the system as a model parameter. The SPC is proven to be a simple yet efficient model for extracting the depth-based lateral resolution as a high-level property of complex plenoptic capturing system.

The contribution of the author to this chapter:

- Evaluating the SPC framework for modelling complex capturing systems such as plenoptic cameras and extracting the high level properties of the capturing system with the desired level of details.

Chapter 7

Conclusions

This chapter provides an overview of the content presented in this thesis work, discusses the outcome of the presented research and offers suggestions for future work.

7.1 Overview

The aim of this thesis work as stated in Chapter 1 is to introduce a framework for the representation and evaluation of plenoptic capturing systems in favour of a unified language for extracting and expressing camera trade-offs in multi-dimensional camera properties space. The motivation for the work in Chapter 1 was highlighted by the developments in the unconventional camera structures including the plenoptic cameras, complexity in definition and extraction of camera properties and existing trade-offs for plenoptic camera properties, the necessity to extract camera properties for design, investigation or evaluation purposes, and lack of the models with the desired descriptive level to extract high level camera properties.

To attain the aim of this thesis work, the SPC framework including a number of constructing modules was initially introduced in Chapter 1. Chapter 2 briefly provided the required background information covering the basic knowledge about capturing systems and, in particular, the plenoptic setup as the focus of this thesis work. The introduction concerning the optical models in Chapter 2 was of assistance in relating the current work at a later stage with other available models.

The details concerning the proposed SPC model were provided in Chapter 3 together with the information regarding how the SPC model is generated through the SPC model generator module in the SPC framework. In Chapter 3, there was a description with regards to how the capturing system is represented in the SPC model and how the focal information, as well as the light field sampling information of the capturing system, is preserved in its SPC model representing.

Chapter 4 illustrated how it was possible to visualize the SPC model and how to benefit from this visualization. Visualizing the SPC model as a set of light cones in

the 3D capturing space in front of the camera and visualizing the $\mathbf{q}-\mathbf{p}$ space representation of the SPC model were discussed as a means to investigating the light field sampling properties of the capturing system.

Discussion in relation to the SPC framework was continued in Chapter 5 where the property extractors to empower the evaluation module in the SPC framework were introduced. The lateral resolution, as a high level camera property was selected to be investigated and three lateral resolution property extractors were introduced that incrementally leveraged on various SPC features.

The SPC model was evaluated in Chapter 6, by applying the introduced property extractors to plenoptic capturing setups and comparing the results with those from established models. Results confirmed the SPC model as an efficient model for extracting high-level properties of the plenoptic capturing system. Through a comparison of the results, the SPC model was also related to the ray-based and wave optics models.

7.2 Outcome

The concept of the light cone as the form of the in-focus light is shown to be useful in modelling the light field sampling behaviour of the capturing system in this thesis work. The fact that the optical transformations in the geometrical optics retain the consistency of the LC as the form of in-focus light element, was of assistance in modelling the light field sampling behaviour of the capturing system using the SPC model. Other modules in the SPC framework, such as the SPC model generator, the visualization module as well as the evaluation module are formed around the SPC model to facilitate the process of actually generating the model as well as showing how it is possible to benefit from this representation.

The first goal of this thesis work, which was to introduce a model to represent the light field sampling behaviour of plenoptic image capturing systems has been completely fulfilled. The introduced SPC model incorporates the ray information as well as the focus information of the plenoptic image capturing system, fully satisfying the second goal of the work. Based on the proposed model, the SPC framework was developed and evaluated and it was capable of extracting the high level properties of plenoptic image capturing systems, fulfilling the third verifiable goal. The outcome of the thesis can benefit design, evaluation and comparison of the complex capturing systems.

”Richer and more realistic assumptions do not suffice to make a theory successful. Scientists use theories as a bag of working tools and they will not take on the burden of a heavier bag unless the new tools are very useful” [58]. If the above quote is applied to the concept of this current work, then it is possible to state that the SPC model and framework can contribute not because it is true, but, because the concept adds to the ray model, notably the focal properties of the optical capturing system, which is thus worth pursuing. The SPC framework is proven to be a simple yet efficient framework for extracting the lateral resolution profile in plenoptic capturing

systems. It is possible to conclude that the SPC framework yields predictions that are straightforward to obtain and are sufficiently detailed for a range of applications.

7.3 Future works

The following is a list of possible tracks for the future work:

- Investigating the validity range of the model is an essential step to take. Defining the exact limitations of the model and the practical parameter ranges in which the SPC framework can provide results with sufficient accuracy requires more in depth assessments.
- The next track to follow is developing other property extractors in the SPC framework. Angular resolution could be a good candidate as a key property in the plenoptic capturing system. To validate such an angular resolution extractor, it might be necessary to have access or the possibility to measure the ground truth data as a reference for comparison. More property extractors will also be of assistance in clarifying the range and scope of the capabilities of the SPC model and framework.
- Another possible track to work on is benefiting from the LCs information such as the base area or the spread of the LCs (on different depth planes) in the image reconstruction algorithms. The knowledge concerning the physical origin of the light samples in the scene could prove to be of assistance in developing better image reconstruction algorithms. A further step in this path could be assigning a content value to each LC and a distribution showing how this content is distributed in the angular span of that LC. If we consider the uniform distribution in the content of each LC, then using LCs to reconstruct the image in a certain depth plain might be comparable to applying a linear interpolation to the images obtained from the ray-tracing algorithms. Other distributions in the LCs might result in other interpolation methods. It is possible to develop a concept of LC-tracing similar to ray-tracing. Images can be reconstructed using LC-tracing and compared with the results from the ray-tracing methods.
- Based on a higher abstraction level (a more abstract level in the system modelling hierarchy), the SPC framework has the potential to be extended to other complex capturing systems. The way that the SPC models the light field sampling behaviour of the capturing system could also be beneficial in other complex capturing systems. The system evaluation capabilities that the SPC framework provides could also be very valuable in complex capturing systems. Camera arrays could be a good candidate for this track. However, the SPC framework might require adjustments for any new capturing system introduced to it. For example, the model generator might require to be revised and the validity of the property extractors for any new capturing system introduced to the SPC framework should be carefully investigated and proper adjustments should be applied.

- Camera evaluation tools, in general, and the SPC framework, in particular, may also permit the study of unexplored camera designs. The SPC framework could facilitate the system evaluation step using, for example, the property extractors that are suitable for interesting high level camera parameters. The SPC framework could be useful in the qualitative and quantitative investigation of the effect of the intentional and unintentional variations of the geometry of the camera system (or fabrication tolerances) on the sampling behaviour and the high level properties of the camera system. The SPC framework could qualitatively show how these variations affect the SPC model (and so the sampling behaviour) of the capturing system, using the visualization module. It could quantitatively reflect the effect of variations in the camera's geometrical parameters on the high level camera parameters of interest using the evaluation module, including the property extractors. The SPC framework could also assist in any insight with regards to how the variations in the camera parameters are reflected in light field sampling behaviour and thus the high level properties of the camera system.

Bibliography

[1] Gary Anthes. Smarter photography. *Commun. ACM*, 55(6):16–18, June 2012.

[2] M. Harris. Focusing on everything. *Spectrum, IEEE*, 49(5):44–50, 2012.

[3] Todor Georgiev, Zhan Yu, Andrew Lumsdaine, and Sergio Goma. Lytro camera technology: theory, algorithms, performance analysis. pages 86671J–86671J–10, 2013.

[4] Anat Levin, William Freeman, and Fredo Durand. Understanding camera trade-offs through a bayesian analysis of light field projections-a revision. 2008.

[5] Ramesh Raskar and Jack Tumblin. *Computational Photography: Mastering New Techniques for Lenses, Lighting, and Sensors*. A. K. Peters, Ltd., Natick, MA, USA, 2010.

[6] Rastislav Lukac and Hayder Radha. Computational photography: Methods and applications. *Journal of Electronic Imaging*, 20(4):049901–049901–5, 2011.

[7] Rachel Ehrenberg. The digital camera revolution: Instead of imitating film counterparts, new technologies work with light in creative ways. *Science News*, 181(2):22–25, 2012.

[8] H. Hoshino, F. Okano, H. Isono, and I. Yuyama. Analysis of resolution limitation of integral photography. *J. Opt. Soc. Am. A*, 15(8):2059–2065, Aug 1998.

[9] Anat Levin, WilliamT. Freeman, and FrÃ©do Durand. Understanding camera trade-offs through a bayesian analysis of light field projections. In David Forsyth, Philip Torr, and Andrew Zisserman, editors, *Computer Vision ECCV 2008*, volume 5305 of *Lecture Notes in Computer Science*, pages 88–101. Springer Berlin Heidelberg, 2008.

[10] Z. Kavehvash, K. Mehrany, S. Bagheri, G. Saavedra, H. Navarro, and M. Martinez-Corral. 3d resolution in computationally-reconstructed integral photography. In *Proc. of SPIE Vol*, volume 8384, pages 838417–1, 2012.

[11] Steven J. Gortler, Radek Grzeszczuk, Richard Szeliski, and Michael F. Cohen. The lumigraph. In *Proceedings of the 23rd annual conference on Computer graphics and interactive techniques*, SIGGRAPH '96, pages 43–54, New York, NY, USA, 1996. ACM.

[12] Marc Levoy and Pat Hanrahan. Light field rendering. In *Proceedings of the 23rd annual conference on Computer graphics and interactive techniques*, SIGGRAPH '96, pages 31–42, New York, NY, USA, 1996. ACM.

[13] Marc Levoy. Light fields and computational imaging. *Computer*, 39(8):46–55, 2006.

[14] Ariel Lipson, Stephen G Lipson, and Henry Lipson. *Optical physics*. Cambridge University Press, 2010.

[15] Sir Arthur Schuster. *An introduction to the theory of optics*. E. Arnold, 1904.

[16] John E Greivenkamp. *Field guide to geometrical optics*. SPIE Press Bellingham, Washington, 2004.

[17] Charles Sumner Williams and Orville A Becklund. *Introduction to the optical transfer function*, volume 112. Society of Photo Optical, 1989.

[18] Gershon Elber. Low cost illumination computation using an approximation of light wavefronts. In *Proceedings of the 21st annual conference on Computer graphics and interactive techniques*, pages 335–342. ACM, 1994.

[19] Ramesh Raskar. Computational photography. In *Computational Optical Sensing and Imaging*. Optical Society of America, 2009.

[20] Jos Stam. Diffraction shaders. In *Proceedings of the 26th annual conference on Computer graphics and interactive techniques*, pages 101–110. ACM Press/Addison-Wesley Publishing Co., 1999.

[21] Gordon Wetzstein, Ivo Ihrke, Douglas Lanman, and Wolfgang Heidrich. Computational plenoptic imaging. In *Computer Graphics Forum*. Wiley Online Library, 2011.

[22] Edward H Adelson and James R Bergen. The plenoptic function and the elements of early vision. *Computational models of visual processing*, 1:3–20, 1991.

[23] Oliver Schreer, Peter Kauff, and Thomas Sikora. *3D videocommunication*. Wiley Online Library, 2005.

[24] Se Baek Oh, Sriram Kashyap, Rohit Garg, Sharat Chandran, and Ramesh Raskar. Rendering wave effects with augmented light field. *Computer Graphics Forum*, 29(2):507–516, 2010.

[25] T Fujii. A basic study on the integrated 3-d visual communication. *Ph. D. dissertation in engineering, Dept. Electrical Eng., Faculty of Eng., Univ. of Tokyo, Japan*, 1994.

[26] Jin-Xiang Chai, Xin Tong, Shing-Chow Chan, and Heung-Yeung Shum. Plenoptic sampling. In *Proceedings of the 27th annual conference on Computer graphics and interactive techniques*, pages 307–318. ACM Press/Addison-Wesley Publishing Co., 2000.

[27] Aaron Isaksen, Leonard McMillan, and Steven J Gortler. Dynamically reparameterized light fields. In *Proceedings of the 27th annual conference on Computer graphics and interactive techniques*, pages 297–306. ACM Press/Addison-Wesley Publishing Co., 2000.

[28] T. Fujii. Ray space coding for 3d visual communication. In *Picture Coding Symposium'96*, volume 2, pages 447–451, 1996.

[29] Bennett S Wilburn, Michal Smulski, Hsiao-Heng K Lee, and Mark A Horowitz. Light field video camera. In *Electronic Imaging 2002*, pages 29–36. International Society for Optics and Photonics, 2001.

[30] Bennett Wilburn, Neel Joshi, Vaibhav Vaish, Marc Levoy, and Mark Horowitz. High-speed videography using a dense camera array. In *Computer Vision and Pattern Recognition, 2004. CVPR 2004. Proceedings of the 2004 IEEE Computer Society Conference on*, volume 2, pages II–294. IEEE, 2004.

[31] Yoshikuni Nomura, Li Zhang, and S Nayar. Scene collages and flexible camera arrays. In *Proceedings of Eurographics Symposium on Rendering*, volume 2, 2007.

[32] Ivo Ihrke, Timo Stich, Heiko Gottschlich, Marcus Magnor, and Hans-Peter Seidel. Fast incident light field acquisition and rendering. In *Proc. of WSCG*, pages 177–184. Citeseer, 2008.

[33] Yuichi Taguchi, Amit Agrawal, Srikumar Ramalingam, and Ashok Veeraraghavan. Axial light field for curved mirrors: Reflect your perspective, widen your view. In *Computer Vision and Pattern Recognition (CVPR), 2010 IEEE Conference on*, pages 499–506. IEEE, 2010.

[34] Ashok Veeraraghavan, Ramesh Raskar, Amit Agrawal, Ankit Mohan, and Jack Tumblin. Dappled photography: Mask enhanced cameras for heterodyned light fields and coded aperture refocusing. *ACM Transactions on Graphics*, 26(3):69, 2007.

[35] Ashok Veeraraghavan, Amit Agrawal, Ramesh Raskar, Ankit Mohan, and Jack Tumblin. Non-refractive modulators for encoding and capturing scene appearance and depth. In *Computer Vision and Pattern Recognition, 2008. CVPR 2008. IEEE Conference on*, pages 1–8. IEEE, 2008.

[36] Douglas Lanman, Ramesh Raskar, Amit Agrawal, and Gabriel Taubin. Shield fields: modeling and capturing 3d occluders. *ACM Transactions on Graphics (TOG)*, 27(5):131, 2008.

[37] Todor Georgiev, Chintan Intwala, Sevkit Babakan, and Andrew Lumsdaine. Unified frequency domain analysis of lightfield cameras. *Computer Vision–ECCV 2008*, pages 224–237, 2008.

[38] Gabriel Lippmann. Epreuves reversibles. photographies integrals. *Comptes-Rendus Academie des Sciences*, 146:446–451, 1908.

[39] Fumio Okano, Jun Arai, Haruo Hoshino, and Ichiro Yuyama. Three-dimensional video system based on integral photography. *Optical Engineering*, 38(6):1072–1077, 1999.

[40] Ren Ng, Marc Levoy, Mathieu Brédif, Gene Duval, Mark Horowitz, and Pat Hanrahan. Light field photography with a hand-held plenoptic camera. *Computer Science Technical Report CSTR*, 2, 2005.

[41] Todor Georgiev, Colin Zheng, Brian Curless, David Salesin, Shree Nayar, and Chintan Intwala. Spatio-angular resolution tradeoffs in integral photography. In *Eurographics Symposium on Rendering*, pages 263–272, 2006.

[42] Kensuke Ueda, Takafumi Koike, Keita Takahashi, and Takeshi Naemura. Adaptive integral photography imaging with variable-focus lens array. In *Electronic Imaging 2008*, pages 68031A–68031A. International Society for Optics and Photonics, 2008.

[43] Kensuke Ueda, Dongha Lee, Takafumi Koike, Keita Takahashi, and Takeshi Naemura. Multi-focal compound eye: Liquid lens array for computational photography. In *ACM SIGGRAPH 2008 new tech demos*, page 28. ACM, 2008.

[44] Edward H. Adelson and John Y. A. Wang. Single lens stereo with a plenoptic camera. *IEEE Transactions on Pattern Analysis and Machine Intelligence*, 14:99–106, 1992.

[45] Ren Ng. *Digital light field photography*. PhD thesis, stanford university, 2006.

[46] A. Lumsdaine and T. Georgiev. The focused plenoptic camera. In *Computational Photography (ICCP), 2009 IEEE International Conference on*, pages 1–8. IEEE, 2009.

[47] Todor Georgiev and Chintan Intwala. Light field camera design for integral view photography. Technical report, Citeseer, 2006.

[48] Roger Olsson. *Synthesis, Coding, and Evaluation of 3D Images Based on Integral Imaging*. PhD thesis, Mid Sweden University, Department of Information Technology and Media, 2008.

[49] Sung-Wook Min, Joohwan Kim, and Byoungho Lee. New characteristic equation of three-dimensional integral imaging system and its applications. *Japanese journal of applied physics*, 44:L71–L74, 2005.

[50] Anthony Gerrard and James M Burch. *Introduction to matrix methods in optics*. Dover Publications, 1994.

[51] Kurt Bernardo Wolf. *Geometric optics on phase space*. Springer, 2004.

[52] Mitra Damghanian, Roger Olsson, and Mårten Sjöström. The sampling pattern cube–a representation and evaluation tool for optical capturing systems. In *Advanced Concepts for Intelligent Vision Systems*, pages 120–131. Springer, 2012.

[53] Mitra Damghanian, Roger Olsson, and Mårten Sjöström. Extraction of the lateral resolution in a plenoptic camera using the SPC model. 2012.

[54] H. Navarro, E. Sánchez-Ortiga, G. Saavedra, A. Llavador, A. Dorado, M. Martínez-Corral, and B. Javidi. Non-homogeneity of lateral resolution in integral imaging. *Journal of Display Technology*, 9(1):37–43, 2013.

[55] B. Wilburn, N. Joshi, V. Vaish, E.V. Talvala, E. Antunez, A. Barth, A. Adams, M. Horowitz, and M. Levoy. High performance imaging using large camera arrays. *ACM Transactions on Graphics*, 24(3):765–776, 2005.

[56] E.H. Adelson and J.Y.A. Wang. Single lens stereo with a plenoptic camera. *IEEE transactions on pattern analysis and machine intelligence*, 14(2):99–106, 1992.

[57] Mitra Damghanian, Roger Olsson, Mårten Sjöström, Hector Navarro Fructuoso, and Manuel Martinez-Corral. Investigating the lateral resolution in a plenoptic capturing system using the spc model. pages 86600T–86600T–8, 2013.

[58] D. Kahneman. *Thinking, Fast and Slow*. Penguin Books, 2012.